Rafael Filipe Gouveia Heneni Lopes

Bachelor in Physical Engineering

Experimental Setup and Performance Testing of an Automated Target Characterization System

Dissertation submitted in partial fulfillment
of the requirements for the degree of

Master of Science in
Physical Engineering

Supervisor: Gabriel Schaumann, PhD,
Institute for Nuclear Physics,
Darmstadt Technical University

Examination Committee

Chairperson: Yuri Nunes
Raporteurs: André Wemans
Supervisor: Gabriel Schaumann

FACULDADE DE
CIÊNCIAS E TECNOLOGIA
UNIVERSIDADE NOVA DE LISBOA

September, 2016

Experimental Setup and Performance Testing of an Automated Target Characterization System

This document was created unsing the (pdf)LaTeX processor, based in the "unlthesis" template[1], developed at the Dep. Informática of FCT-NOVA [2]. [1] https://github.com/joaomlourenco/unlthesis [2] http://www.di.fct.unl.pt

Acknowledgements

Firstly, I would like to thank my supervisor Dr. Gabriel Schaumann for giving me the opportunity to work in this project, providing me continuous feedback and the necessary tools and making me feel at home while I was in Germany.

I am also grateful to everyone in the Detector and Target Laboratory for the tips and teachings on how to use some resources, specially Nico Neumann for all the feedback and knowledge he gave me on electro-mechanical systems, Tina Ebert for helping me understanding the basics of communication between LabVIEW and the Point Confocal Sensors, and Torsten Abel for the help and tips he gave me for using a camera with LabVIEW's VISION package.

I would like to thank Erasmus+ program for giving me the amazing opportunity and resources for doing my dissertation in Germany.

I thank FCT-UNL for all the knowledge that was passed to me during my degree, including all the great teachers I had the pleasure to meet and the colleagues I managed to befriend, and TU Darmstadt for receiving me so well during my exchange program.

My sincere thanks to everyone that was involved in my exchange program, specially the International Offices of both FCT and TUD that helped with so many questions and problems, and all the people I met and made me feel at home in Darmstadt.

Finally, a big thanks to my friend David Lopes for giving me encouragement and support during this important period, and to my family's support that made all of this possible.

Abstract

Different physical experiments nowadays require the usage of a target onto which a laser or particle beam is focused. A target characterization becomes very important before using them in experiments to make sure their surfaces topography and thickness are within a range of expected values for the experiments.

To characterize the targets produced in the Detector and Target laboratory at the Institute for Nuclear Physics at the University of Darmstadt an automated system based on optical metrology was developed. Using optical Point Confocal Sensors and motors controlled by a LabVIEW application it is possible to characterize targets with a lateral resolution up to 4 μm with sub-micron thickness precision.

The whole scanning system is more efficient in terms of time and accuracy due to its automation and the optical sensors compared to the previously used method that made use of physical contact scanning and was not automated.

The solution developed within this work has some basic functionalities allowing the user to define some scanning parameters, but more functionalities specially related to the Point Confocal Sensors can be developed to allow a more customizable and efficient scanning.

Keywords: Optical Metrology, Automated System, Target Characterization, Point Confocal Sensors, LabVIEW

Resumo

Diferentes experiências físicas requerem nos dias de hoje alvos para focar feixes laser ou de partículas. Uma Caraterização de Alvos torna-se muito importante antes de serem utilizados em experiências, para garantir que a topografia das suas superfície e espessura estão dentro do intervalo de valores esperados para a experiência.

Para caraterizar os alvos produzidos no laboratório de Detetores e Alvos no Instituto para Física Nuclear da Universidade de Darmstadt, um Sistema Automático baseado em Metrologia Ótica foi desenvolvido. Utilizando Sensores de Ponto Confocal e motores controlados por uma aplicação LabVIEW, é possível caraterizar alvos com uma resolução lateral até 4 μm com uma precisão na ordem do sub-micron.

Todo o sistema de varrimento é mais eficiente em termos de tempo e precisão devido à sua automatização e sensores óticos, comparado com o método anteriormente utilizado que envolvia contato físico com o alvo e não era automatizado.

A solução desenvolvida está pronta para usar com algumas funcionalidades básicas, permitindo o Utilizador definir alguns parâmetros de varrimento, mas podem ser desenvolvidas mais funcionalidades, relacionadas especialmente com os Sensores de Ponto Confocal por forma a obterem-se varrimentos mais eficientes.

Palavras-chave: Metrologia Ótica, Sistema Automático, Caraterização de Alvos, Sensores de Ponto Confocal, LabVIEW

Contents

List of Figures

List of Tables

Glossary

COM Communication port on a computer to communicate with other devices.

LCD Liquid Crystal Display.

LED Light Emitting Diode.

USB Universal Serial Bus.

Acronyms

AD Acceleration Distance.

AP Actual Position.

AR Axial Resolution.

CMM Coordinate Measurement Machine.

i Cell_X.

IP Initial Position.

j Cell_Y.

LSX Linear Stage X.

LSY Linear Stage Y.

LSZ Linear Stage Z.

LV LabVIEW.

MA Measuring Angle.

MP Master Probe.

MR Measuring Range.

MX Motor X.

MY Motor Y.

MZ Motor Z.

n Refractive Index.

NA Numerical Aperture.

PCS Point Confocal Sensor.

PTM Position to Move.

RD Reference Distance.

ROI Region of Interest.

RS Reference Standard.

SD Spot Diameter.

SH Sample Holder.

SoS Speed of Scan.

SP Slave Probe.

SR Scan Rate.

WD Working Distance.

Chapter 1

Introduction

The main goal of this project is the development of a Coordinate Measurement Machine (CMM) using two Point Confocal Sensors (PCSs) to acquire data of the geometry of micro-components. It is expected to measure a spatially resolved thickness distribution of samples with an accuracy better than 1 μm over a lateral range of 1 mm. The measurement of the lateral range is only limited to the motion system that positions the samples.

The system should be automated with LabVIEW (LV) integration providing options for setting up target specific measurement routines and obtaining data about the samples geometry, e.g. a thickness distribution map.

This CMM is to be developed accordingly to the needs of laser-accelerated ion experiments that use a high intensity laser pulse, focused on a thin foil (the target), that accelerates ions from the rear target surface within a few micrometers to energies in the MeV range. The target thickness and the surface quality of the rear target side are for this reason some of the most important characteristics for obtaining better results. The targets used in these experiments can have several shapes and have different fabrication techniques involving the addition, shaping and removing of material.

Each of the fabrication procedures have errors associated and they require the characterization of the resulting samples to assure they have the minimum conditions for the experiments[1]. Different techniques for the sample characterization have different accuracy and resolution influencing the errors of the sample characteristics. Some samples require very precise measurements and some techniques can be harder to apply for the characterization.

With the previous measurement method, that involved physical contact (similar to a Vernier caliper), there was the disadvantage of requiring a carefully chosen contact force (dependent of the material), otherwise it could damage the sample.

In comparison, an optical measurement has more advantages in terms of Speed of Scan

(SoS). Techniques like white light interferometry, confocal microscopy or atomic force microscopy can be used in the laboratory. For example the atomic force microscopy can use very fine tips, e.g. a radius in the order of the nanometres, which do not necessarily require high contact forces, permitting measurements with very high accuracy without damaging the sample. However, this technique is slow and with the actual setup at the laboratory it can only measure from one side.

The thickness accuracy of the used targets in investigation should be 1 μm or better, with a lateral resolution of 5 μm or better, that depends on the Spot Diameter (SD) of the optical probes and motors used. The data received from this area is then averaged to a single point to create distribution maps, e.g. thickness distribution (Figure 1.1). The actual surface roughness is measured with different techniques, e.g. Atomic Force Microscopy or Optical Confocal Microscopy[1], as it implies a small scale length. With the CMM it is possible to obtain information about the general shape (larger scale).

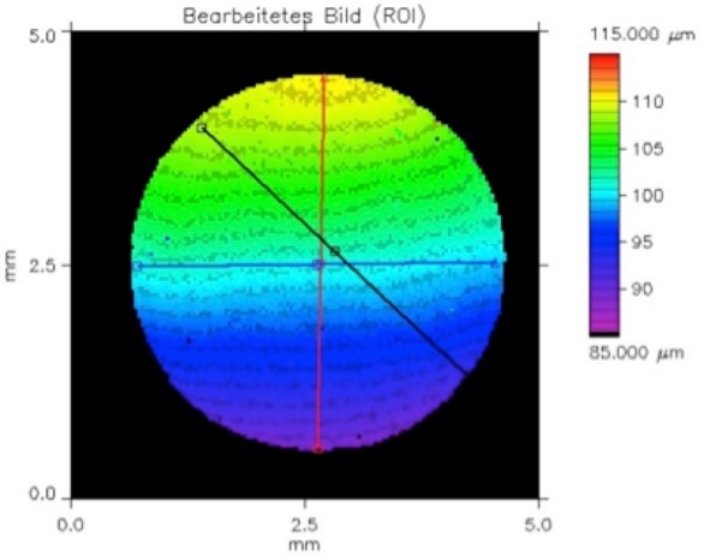

Figure 1.1: Exemplary thickness distribution map

(Source: Dr. B. Kindler, Target Laboratory, GSI).

In a three-week experimental campaign a typical number of targets is 50-100 with current high energy, high intensity laser systems that can, in average, deliver a shot every 30 min. At present there are a few laser systems (large scale machines) with high intensity and medium energy that can deliver a shot once every 40 minutes, e.g. the Phelix Laser System[2] at GSI (Gesellschaft für Schwerionenforschung) Helmholtz Center for heavy ion research located a few kilometres from Darmstadt. Currently there are many high intensity systems built with higher shot rate that can deliver pulses once every minute up to 10 Hz making it necessary to increase the speed of the processes in the target fabrication and characterization.

With the CMM the time efficiency improves due to the automated process and it is possible to get a better accuracy due to the motion system and the optical sensors. In

addition, it tracks more data of the target and the system conditions that can be used to perform software compensations and obtain more realistic information.

Chapter 2

Three-Dimensional Surface Topography

The developed CMM requires the understanding of some three-dimensional (3-D) surface topography concepts and existing techniques. The chosen technique was done based on the different characteristics of the available instruments and components[3].

Firstly it is necessary to understand the differences between 2-D and 3-D surface topography. 2-D scanning doesn't provide enough information about the surfaces topography for the applications of the samples used. In contrary, 3-D scanning can provide more meaningful parameters due to a more independent data acquisition and the proximity of its characteristics to the 3-D reality nature[3]. Even though the costs of the instrumentation tend to increase for 3-D scanning, its good resolution, accuracy and more informational data are required for this project.

At the present there are different available methods and instruments for 3-D surface scanning. Due to the need of maintaining the samples intact, non-contact instruments are required. From this classification, optical working methods are often used in surface metrology specially due to their non-contact characteristics and speed of measurement[4].

2.1 Optical Systems

For the reasons previously mentioned an optical system was preferred for this project. Interferometry and focus detection are two of the most used principles in optical instruments[5].

Interferometry: Two light waves interfere with each other and produce fringes that relate with constructive and destructive, allowing the detection of very small distances.

Focus detection: A light wave is reflected by a dichroic mirror and focused by an objective lens to a small spot of a surface. Variations of height in the surface can

be identified by moving the lens or the sample to keep the focusing spot constant, while measuring the variation of these motion. In the specific case of the confocal method the principle is to eliminate all the light that is out of focus, by inserting two pinholes that have a same focus in the sample[3, 5].

2.2 External Factors

Vibration can affect the data acquisition since any motion of the components will decrease the position accuracy: if the motors vibrate, the motion passes to the linear stages, to the carriers and to the Sample Holder (SH); if any of the optical probes moves the accuracy position will again suffer since the focus relates with a different position in the sample. With the different axis existing in the system and depending on the materials and the environment conditions, a small vibration can lead to a position error of an undesirable order so the characteristics of the used components should be taken into account[6, 7].

Temperature can influence extension and elongation of all the components of the CMM and of the samples. When analysing the optical system, temperature can easily affect the results, since small changes in lenses and mirrors lead to a change of the path of the light providing bigger differences for small temperature variations. Since the optical probes have lenses and mirrors, temperature variation affects the focus of the LED inside the probe; when the light reaches the surface, depending on the material, the reflectivity will be changed, giving different data; the reflected waves will then arrive again at the probe, which once again will pass by an optical system[7] also includes temperature influence.

Chapter 3

Mechanical Design

For the mechanical design of the system 5 sections were considered: the PCS's, the motion system, the supporting structure, the positioning camera and the compensation system. The developed design for this project can be seen in a simplified version in Figure 3.1. The different components are explained in this chapter.

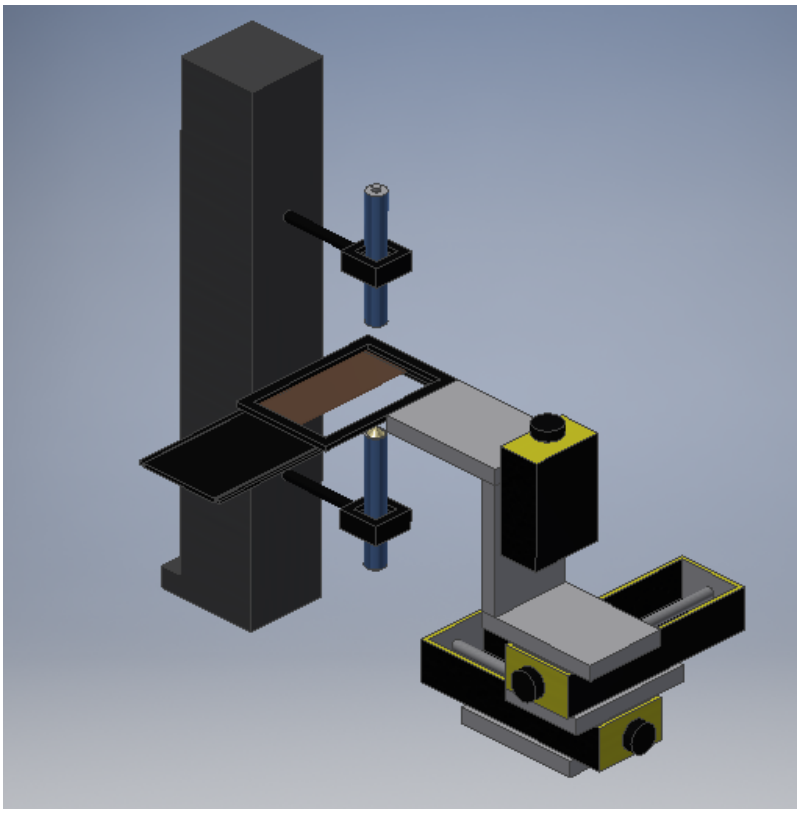

Figure 3.1: Simplified ortographic view of the developed mechanical system designed with Autodesk® Inventor LT™.

3.1 Point Confocal Sensors

Two PCS's (See Figure 3.2) are used in the CMM, each of them connected to one probe (See Figure 3.3) by optical fibers, one staying above the SH and one staying under, Master Probe (MP) and Slave Probe (SP), respectively. The optical probes used have a length of 125 *mm* and a diameter of 19 *mm*. The PCS's have a great importance in the mechanical design. For this reason it is crucial to understand the functionalities, properties and limitations of these sensors.

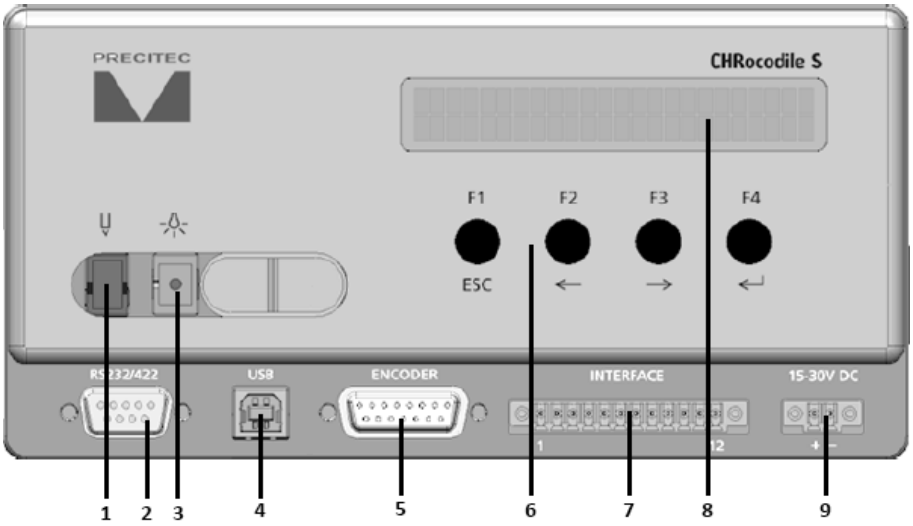

Figure 3.2: General view of the optical sensor CHRocodile S: 1-Optical fiber connection port; 2-RS232/RS422 Serial Interface; 3-External light source port; 4-USB port; 5-Encoder Input; 6-Function buttons; 7-Multi-point interface connector; 8-LCD; 9-Main power supply Jack.

Figure 3.3: 600 μm optical chromatic probe designed with Autodesk Inventor LT.

3.1.1 Working Method

The probes used in this project make use of the physical principles optical emission and reflection. Each of them has a broadband light source (LED) that emits light through an

optical fiber tree coupler. After the light leaving the fiber it goes trough an hyperchromatic lens that focus the existing wavelengths onto different planes at different distances of the sensor. One of these wavelengths reaches the surface of an object with a certain SD and is reflected back to the optical fiber inside the probe; only a small percentage of the other wavelengths will get back to the optical fiber. A spectrometer receives the reflected wavelengths, from which the maximal intensity (highest peak) gives a value for the corresponding distance due to its proportionality[8, 9]. The simplified process can be observed in Figure 3.4(a). The sampling for the spectrum is done at a minimal step of 20 *nm* - the Axial Resolution (AR) -, that depends on the relation between the wavelength range (400-750 *nm*) and the Measuring Range (MR): for the same wavelength the broader the MR the smaller the AR. The spectral response of the spectrometer also influences the resolution of the measurements, mainly when there is motion involved. In the case of no motion, a value would be measured in a ±20 *nm* range.

In the case of a transparent material, two groups of wavelengths will be reflected, one belonging to the first surface and the second one to the second surface, being the second one less intense due to losses through the material as seen in the Figure 3.4(b).

There is an interferometric method, which is capable of measuring up to 3 different thicknesses simultaneously with at least 2.5 μm for each of them[10]. This method requires a known Refractive Index (n) and it uses a different probe for interferometry. This method highly depends on the quality of the signal and can be specially used for multiple layers samples.

In this project only the method that uses a single surface is used, as the samples to scan are non-transparent and the usage of 2 sensors can decrease the error compared to the 2 surfaces method, in which case the light intensity of the second surface would lose intensity when passing through the material and and the second surface detection is dependent of the MR of the optical probe used. Also the n is usually not known and the quality of the interferometric method would be a problem for certain materials and thicknesses.

3.1.2 Specifications

The two indentical sensors used in this system were acquired from Precitec Optronik GmbH[11], which provides a manual for CHRocodile S with 2 kHz technology[10] with a list of different options, commands and specifications (See Table 3.1).

The Working Distance (WD) and the MR are two of the most important characteristics for this project. The WD is the distance from the bottom of the probe to the middle of the MR, the latter being the range from which the probe can take data. The probes can take information from a surface positioned in the range of WD±MR/2. From the Table 3.1 for the chromatic method with a WD as 6.5 *mm* and a MR as 600 μm this gives a range 6.2-6.8 *mm*. It was noticed during the measurements done that the sensors could measure up to about 660 μm instead of the 600 μm mentioned in the manual, so in practice it is possible

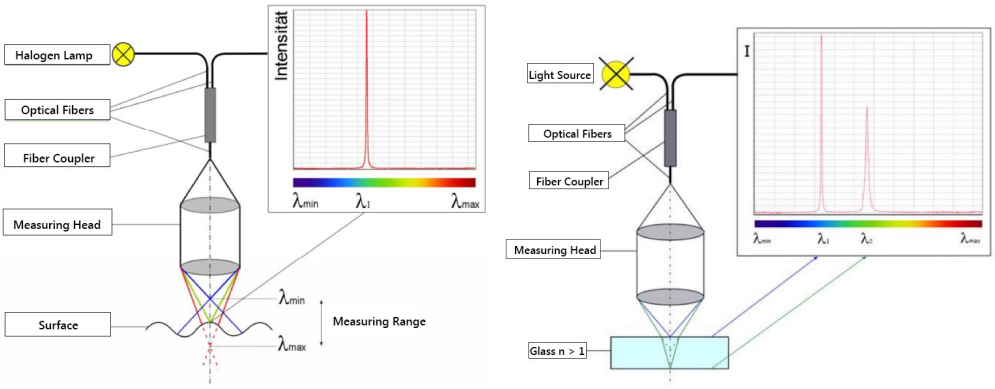

(a) 1 Surface Mode. (b) 2 Surfaces Mode.

Figure 3.4: Working methods of the sensor Probes

(Source: Precitec Optronik GmbH, Optical Sensor CHRocodile S Operation Manual).

to extend the range to 6.17-6.83 mm.

The SD is related with the lateral resolution: the smaller it is, the better the resolution of the system.

Numerical Aperture (NA) and Measuring Angle (MA) are conditioning characteristics for the size, shape and material of the samples to be analysed. The NA depends on the n of the lenses and the angle θ of the light cone that enters or exits the lens defined by

$$n \times \sin\theta = NA \tag{3.1}$$

Table 3.1: Specifications of the 600 μm probe for the chromatic mode[10].

Specifications	WD	MR	SD	LR	NA	MA	AR
Value	6.5	600	4	2	0.5	90+/-30	~20
Units	mm	μm	μm	μm		o	nm

3.2 Motion System

Three stepper motors are used together with linear stages to position the SH in the XYZ coordinates during the scanning and pre-scanning process. Motor X (MX) and Motor Y (MY) are used to move the SH in the XY plan parallel to the base surface together with Linear Stage X (LSX) and Linear Stage Y (LSY), respectively. To position the SH between the two PCS it is used Motor Z (MZ) together with Linear Stage Z (LSZ) in the Z-axis, perpendicular to the XY plan previously mentioned.

The motors and linear stages used during the tests of this project were used as a whole component, already prepared to automatically do conversions from rotational to linear motions.

3.2.1 Stepper Motors

Stepper motors are electromechanical devices that convert electrical pulses to a rotational motion defined by a number of discrete steps. The higher this number of steps, the greater the resolution. It is common for stepper motors to have steps of 1.8° corresponding to a total of 200 steps for 360°, but other values can be found in the market[12, 13].

This type of motors is very used for motion control. With the help of a rotational encoder, it is possible to better characterize the motor state, e.g. the speed of rotation and the step that it currently is at that can be converted to a linear position. This is one of the reasons this type of motors is a good choice for this project. With the need of a better resolution of a positioning system, the rotational distance corresponding to one step can be reduced, but smaller steps lower the accuracy of the read value since it is harder to measure smaller motions with the encoders, together with the decrease of the available torque [12, 13, 14].

To increase the resolution there are two techniques available: half-step and microstepping. For half-step the motor alternates between single and dual-phase, which allows an half-step between two neighbour phases, doubling the resolution; microstepping makes use of a sinusoidal waveform for power switching, resulting in smaller steps that are a division of the original ones resulting in an increase of the resolution by a factor of 10 to 256 and a smoother operation[13, 15]. Microstepping increases resolution, but it can have some disadvantages. Due to differences between a pure sine curve and the real position of the shaft, the accuracy lowers. Torque will also be affected needing in some cases (depending on the load) to execute more than one microstep[16].

3.2.2 Linear Stages

Linear stages are used to restrict the motion of objects to one single linear axis manual or automatically. Actually there are very precise industrial linear stages in the market with resolutions in the order of the nm, e.g. some linear stages from SmarAct[17]. However, due to the high-costs of such devices, usually in the order of thousands of euros, it is preferable the development of a customized linear stage. Even though the current version of the CMM makes use of three acquired linear stages similar to Figure 3.5 that already existed at the laboratory, some research was done towards the development of linear stages.

For each of the linear stages a certain translation range is required. In the X- and Y-axis they depend on the biggest expected width and height of a sample to scan. The values of 100 *mm* were considered reasonable since the samples have usually a width no bigger than 80 *mm*, providing some extra available width for future needs. Since the samples are usually rectangular and one of the sides is smaller, a value of 50 *mm* for the smaller side could be used. In the case of the Z-axis linear stage, a much smaller range is required, as it is dependent of the maximum thickness the system is expected to measure. Also, it

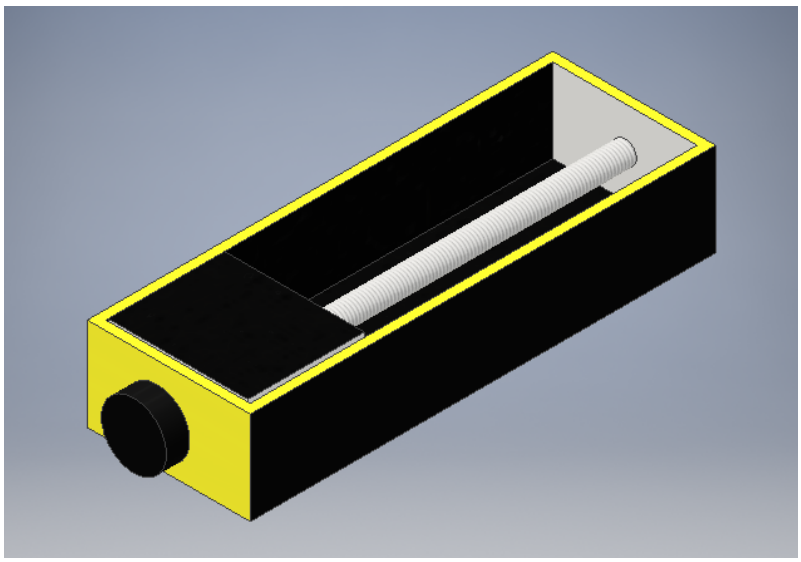

Figure 3.5: Linear stage with a motor used during the tests designed with Autodesk® Inventor LT™.

requires a higher precision than the XY stages since it affects the thickness measurements. A value of 5 *mm* is sufficient for this stage.

The resolution of a linear stage depends on the step size of the stepper motor and the repeatability depends on the friction between the rail bearings and the carriage. The performance depends on the type of bearings used.

To convert the rotational motion to linear it is required a linear actuator, usually a leadscrew. Its size depends on the translation range required. The diameter influences the speed of rotation and the required torque. The thread/tooth shape and height influence the gap between the carriage connection and the leadscrew, influencing vibration. The distance between two teeth - the pitch - affects the linear resolution and linear speed: more threads per *mm* means a better resolution but lower speed[18].

Initially the linear stages were used manually with the motors turned off to test the PCS's. With information of the motors' step position and the dimensions of the linear stage components it is possible to get a value for the linear position in the stage.

3.2.3 Backlash

Mechanical backlash is a very common problem in mechanical devices. It results from the gaps between the drive and driven gears. The teeth require a certain space in order to avoid high tensions between both gears, otherwise a stronger force would be required to move the gears.

Backlash becomes specially important to high-precision positioning systems as its influence becomes more noticeable due the smaller moving steps being in an order closer to the backlash. Even though the backlash is dependent of the gears and screws, due to

the difficulties in manufacturing better systems it is necessary to find options to reduce its effect on the data taken.

In a scanning system it is common to have the motors move the carriers back and forth. Looking at the Figure 3.6 when a carrier would be moved in the positive motion, the drive gear as it's already in contacts with the driven gear would immediately start moving it. However, when the drive gear would move in the negative motion, it would first have to move the backlash distance and only after it would start moving the driven gear. This would give a wrong read position with a difference corresponding to the backlash distance.

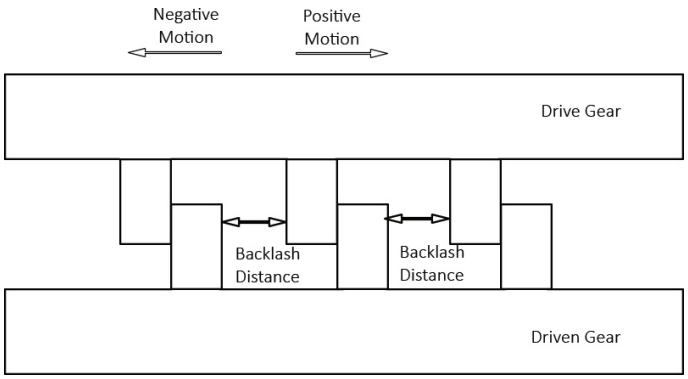

Figure 3.6: Backlash in a mechanical system.

3.2.4 Encoders

Problems like the backlash and small steps of the motors can affect the accuracy of the measurements. With the usage of encoders it is possible to reduce the influence of these problems, as they can directly read the rotational or linear position (with a rotational or linear encoder, respectively), instead of just assuming the position accordingly to the number of steps sent to the motor and the conversion of the assumed value to a linear position.

The motors used in this project have a rotational encoder that can measure the position of the motor spindle relatively to the coils. In case there is some possible resistance that, e.g. would make the spindle not move, the discrepancy between the number of performed steps and the commanded steps would be detected.

The used linear stages have no linear encoders, which requires the conversion of the rotational encoders read values to a linear position. These values are dependent of the relation between the motor spindle and the linear stage spindle so if, e.g. the connection between them breaks or there is some motion in a different axis, the actual position can't be read and is assumed as the converted value. For these and other reasons the usage of linear encoders can improve the precision of the linear position since they read values in a linear scale.

Even though the linear encoders were not yet implemented, some research was done about some possible options for the project. Encoders can be classified by the output as incremental or absolute: incremental encoders work based on 2 phase-shifted, square-wave signals and can be used when a reference position is needed, e.g. the beginning of the scale, to which all the marks of the scale are associated; absolute encoders measure directly the value of a position, not requiring reference values, and the output works in digital bits[19, 20].

Encoders can also be classified in terms of physical principles. Optical encoders usually have a glass scale patterned with transparent and opaque areas that can be detected if put in the middle of a light source and a photodetector (scanning unit); magnetic encoders make use of a magnetic scale, in which the magnetic field changes with a magnetic head and these changes are detected by a magnetic sensor that can associate with a position along the scale[19, 21].

3.3 Supporting Structure

The CMM is supported by a solid vertical structure that has two small components to hold the optical probes and manually position them with high precision.

The motor stages and the vertical structure are connected with screws to a platform that is capable of counter balancing changes in weight.

3.4 Typical Sample

In the CMM a typical sample for scanning is defined by the parameters Region of Interest (ROI), number of regions N (=$N_X \times N_Y$) in the sample, distance between cells (Steps) and the Reference Coordinates.

1. ROI_X: Dimension of a Cell in the X-Axis.
2. ROI_Y: Dimension of a Cell in the Y-Axis.
3. N_X: Number of Cells per horizontal cell's line of the sample.
4. N_Y: Number of Cells per vertical cell's line of the sample.
5. $Steps_X$: Distance in the X-Axis between the same corner point of two different neighbour Cells in the same horizontal cell's line.
6. $Steps_Y$: Distance in the Y-Axis between the same corner point of two different neighbour Cells in the same vertical cell's line.
7. Reference Coordinates: Coordinates of the center of the first cell to be scanned, with the (0,0) point in the corner of the sample.

3.4.1 Sample Holder

The SH seen is the component where the samples are placed and later moved by the motors to the Initial Position (IP) of the scan. In the actual design the user can put a single sample, requiring a manual operation: first the Reference Standard (RS) is placed and a Reference Distance (RD) is taken with the program; then the RS is substituted by the sample to scan. The SH stays between the two optical probes MP and SP within the WD and the MR of both of them. This depends on the thickness and shape of the sample to scan, since the RD will change with different thicknesses. A hypothetical SH was developed as seen in Figure 3.7

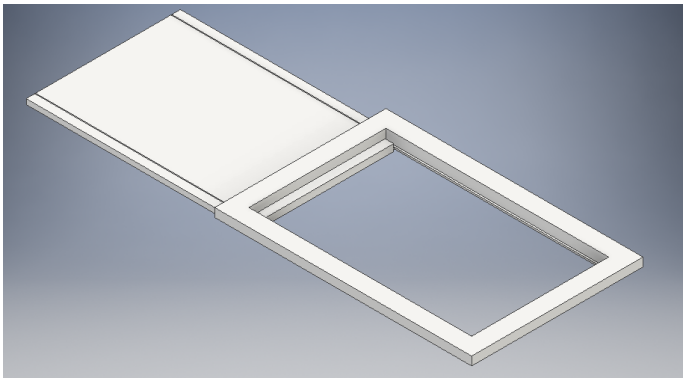

Figure 3.7: Developed sample holder with movable base designed with Autodesk® Inventor LT™.

3.4.2 Sensor Holder

The optical probes are hold by one holder each, similar to Figure 3.8. These holders are also used to position the probes with high-precision in different axis, specially useful to manually calibrate the focus of both of the probes..

3.5 Positioning Camera

The positioning camera should stay next to the MP and is used to search for the point of the sample where the scanning should start. The user selects the corner in a picture obtained by the camera and the motors activate automatically to positioning the sample in the IP, taking the relative distance from the camera to the MP and the SH and the pixels of the image corresponding to the selected corner.

In case the shape of the sample has no vertices, the camera VI could virtually create a circumference based on the given ROI values (or an estimated diameter value) and a virtually measured angle of the identified shape like in Figure 3.9. Knowing these two values, the center of the circumference C can be estimated as (R,R), with R=ROI/2 from which a rectangle is created and the initial point O of the virtual sample is given by (0,0).

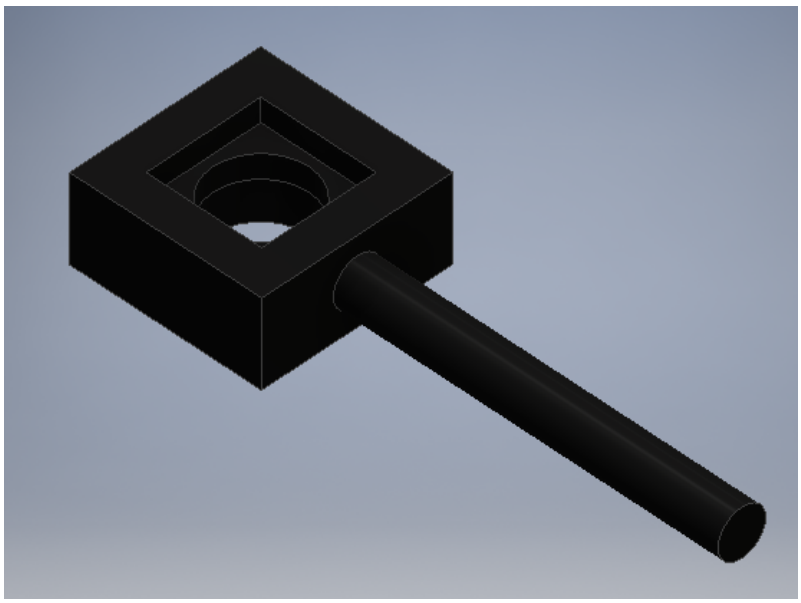

Figure 3.8: Simplified shape of a sensor holder. Image designed in *Autodesk Inventor LT*.

The dimensions of the rectangle would be 2R×2R in case of a square and assuming that the program would perfectly identify the shape. However, due to errors associated to the virtual measurement of the angle, a percentage of about 5% should be added to the expected dimensions, to guarantee that the whole elliptical sample is included in the virtual rectangle sample.

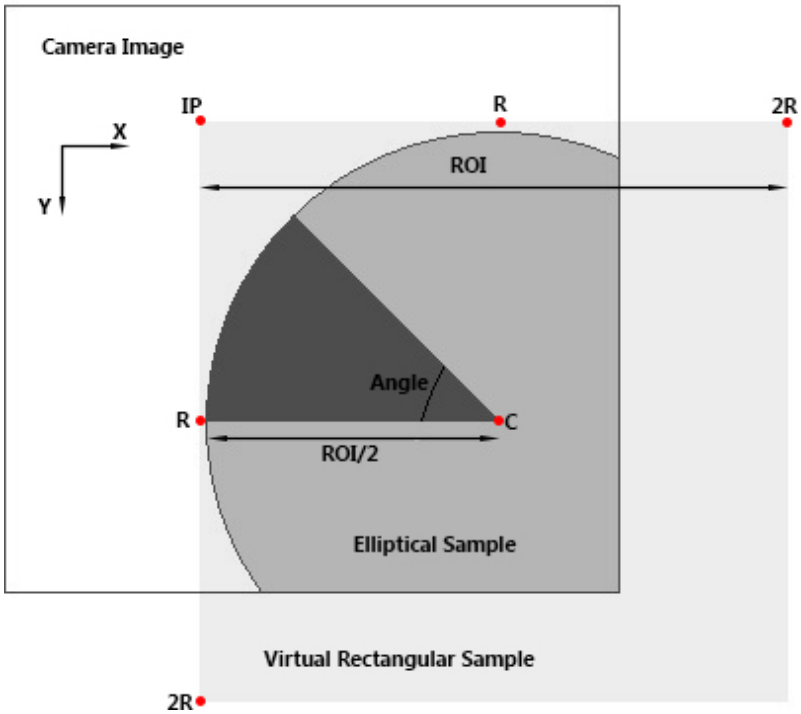

Figure 3.9: Example of elliptical-shape samples detection with the positioning camera.

3.6 Compensation System

To compensate variations of temperature and vibration in the system and reduce errors due to their influence, external sensors can be used to measure these parameters. The data can be received by the computer that performs a software compensation, reducing the error contribution from these parameters.

Most of the vibration that can influence the results is due to the teeth of the linear actuator. Since the CMM doesn't use very fast motions, the frequencies are expected to be low. However, it's still recommended the control of vibration, specially for longer scans, where unexpected vibrations can give origin to wrong measurements.

For vibrational measurement an accelerometer can be used in the SH. Accelerometers are sensors that measure dynamic acceleration as voltage, usually making use of the piezoelectric effect. This effect results from the change of the electrical polarization of a material that is subjected to mechanical stress[22]. There are many different accelerometers available in the market. One of the most important factors for the selection of the right accelerometer is its sensitivity that relates vibration with voltage for a reference frequency[23, 24].

3.7 Relative Distances

It is necessary to know the Relative Distances between some of the components, as they will be used by LV to decide where to move the SH within the safety range and with the best accuracy.

•Z carrier to surface

•SH to Z Carrier in Z-axis

•SP to surface

•SH to X carrier in X-axis

•SH to Y carrier in Y-axis

These distances might change over the time and with the usage, most of which can be corrected with Software calibration (See Section 4.4). However, some of these values might require a manual calibration from the user (or even from the factory), e.g. if it is needed to move some of the probes in the XY plane, since there are no motors controlling them in this CMM version.

3.8 Operating Details

Before using the software to control the CMM it is recommended to take a few steps in order to have the best performance.

The first thing to do is to make sure the sensors are well connected to the probes by the optical fibers and to the computer through the right COM ports. Switching the MP and the SP will provide thicknesses with the wrong values, so it is crucial to verify this detail. For the safety of the components it is also important to verify that the motor cables are not switched, at the risk of damaging the Linear Stages due to passing the limit distances or even the SH, samples and the probes specially with MZ. It is also recommended to make sure no cables are or can be in the way of the motors' carriers or between the probes, with the risk of getting wrong data and/or damaging the cables.

Having these points verified, the user can turn ON the PCS's with the two existing buttons, one for each of them, and the motors drivers. Precitec manual recommends to wait 10 minutes for the LEDs warm-up.

The optical probes can be manually adjusted in the case of their removal or to calibrate the position of the focus of both probes. The latter can be done with the help of the values read in the sensors: if the sensors don't show data taken from the same point simultaneously, then it is required to move one of the sensors in the XY plane with the help of the controllers until the data is acquired at the same point.

While the software is running the components should not be turned OFF with the risk of damaging them. During this phase it is only required to manually adjust the MP on the Z-axis depending on the sample to be scanned, being everything else automatic or controlled with the LV program.

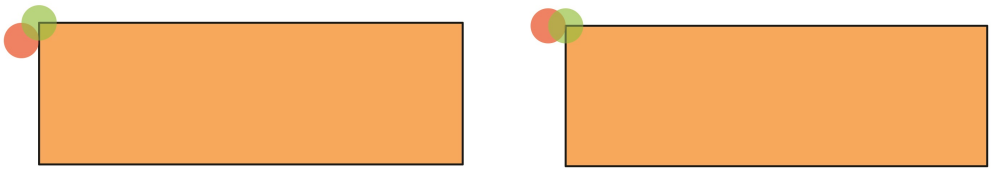

(a) Calibration needed in the X- and Y-axis.

(b) Calibration needed in the X-axis.

(c) Calibration needed in the Y-Axi.

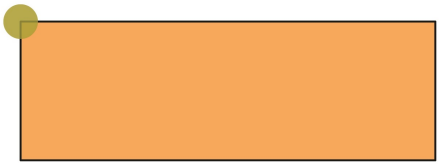

(d) No calibration needed.

Figure 3.10: Cases requiring manual adjustments of the optical probes' position in XY plane (3.10(a),3.10(b) and 3.10(c)) and calibrated case (3.10(d)).

Chapter 4

LabVIEW

During the period of development of this project the major focus was made in the LV integration: each of the components have to work in synchronization and execute different functions, both independently and in parallel, which requires a stable and well-designed application[25] which resulted in a VI hierarchy (see Annex 7.1).

Each of the devices used have their own commands, some with their own subVIs which requires the knowledge and understanding of different LV functionalities such as data communication and synchronization. The dimensions and properties of the mechanical design had to be taken in consideration to guarantee that the equipment and samples would not be damaged during the different tests performed with the software.

The main VI is divided in three *while* cycles that work in parallel when the program starts to run: the events cycle, motors cycle and operations cycle. The event cycle is used to detect value changes and buttons pressed by the user. It is connected to the operations cycle by a queue and, whenever an event is triggered, it adds a constant to the queue that later activates the case in the operating cycle corresponding to the value received.

The operations cycle is only used after an event is triggered, in which case the code associated to the event is executed in this cycle. It executes most of the code of the application.

The motors cycle is controlled via notifications, by the aforementioned cycle. The operations cycle sends notifications to this cycle with an associated constant. This constant is then used to select the case to operate, e.g. to move the sample with MX and MY to a new position.

4.1 Interface

The interface is composed by three main boxes: one at the top-left one to start and exit the program; one at the bottom-left dedicated to the pre-scanning functions; and one at the right for data visualization. Each of these boxes have their own different functionalities and should be used in a specific order. This section explains how to use the interface in order to understand the inputs needed and the expected results of the scan.

4.1.1 Start and Exit Box

Before the initialization (Figure 4.1) there is an option to choose the data of the Telegrams as ASCII or binary, in which the ASCII is used as standard. The binary option was added for future development, but is not functional in the current version. Before pressing the *Initiate* button the user should confirm that the COM ports associated to the Master and Slave sensors and the motors are correctly selected. A refresh of the visible COM ports might be needed in case the USB cables were recently removed.

Pressing the *Initiate* button keeps the button as LOW and changes the text to *Initiating*, starting the initialization algorithm for the PCS's (see Annex 7.2). When finished, the text of this button changes to *Finished* and the LED next to the button turns ON, meaning the initialization of the program is complete and it can advance to the next step.

In case the initialization does not work like previously described, e.g. the LED not turning ON or the text of the button not changing to *Finished*, the button *EXIT* should be pressed in order to exit the program. In this case the user should then confirm that the devices are well connected and once again verify the COM ports in the program. Sometimes due to previous errors occurring in the program during the same session, some variables might be kept in memory and give origin to unexpected results. A restart of LV or even of the computer might be required in this case.

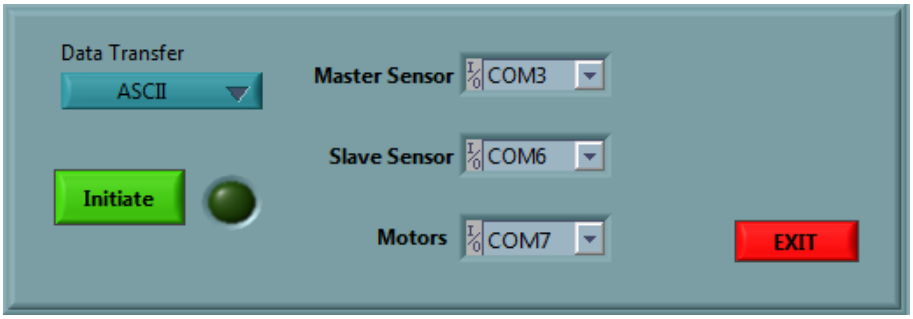

Figure 4.1: Start and exit box.

The button *EXIT* should be the button used to exit the program at any time and not the LV *Abort Execution* button in the Front Panel, the user being advised not to directly press the *EXIT* button while a scan is ongoing.

4.1.2 Pre-Scan Box

After the initialization phase is finished, the user can proceed to the pre-scan box. This box is divided in four tabs that should be used in order from left to the right:

Optical Sensors: The tab seen in Figure 4.2 is dedicated to the configuration of the optical sensors. In the actual version of the program the user can change the *Scan Rate*, the *Data Averaging* of the sensors, the *Refraction Index* of the sample and the *Measuring Mode*, but only the *Scan Rate* (see Annex 7.3) and the *Data Averaging* are effectively working, as the others were used only for testing and kept for future development. Each time the user changes a parameter in this section, a command is sent to the sensors with the new Input and the values of the columns *Master Sensor* and *Slave Sensor* are updated accordingly to the new values. The *Min SR* parameter is defined by the resulting values of a *Dark Reference*, these depending on the intensity of the light sources of the optical probes and on the room light. In case this reference is taken, it might be needed to use again the *Optical Sensors* tab to change the Scan Rate (SR).

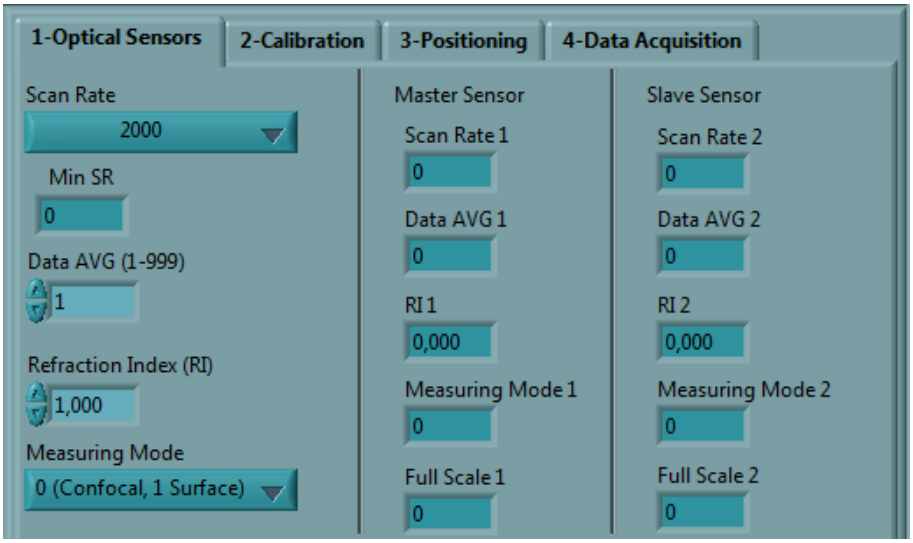

Figure 4.2: Optical Sensors tab.

Calibration: The calibration tab seen in Figure 4.3 is meant to calibrate the PCS's and the motors in order to obtain data with better accuracy. For the PCS's a *Dark Reference*, a *Light Adjustment* or a *White Reference* can be performed. For the motors their carriers are *Homed* to remove errors due to previous motion during an OFF state.

Positioning: The positioning tab seen in Figure 4.4 is used to position the sample automatically or manually. In the automatic option it uses the non-implemented positioning camera to position the sample in the XY-plane and to make the Z-axis focus with *Focus Z*. The reference distances between the sensors and the sample

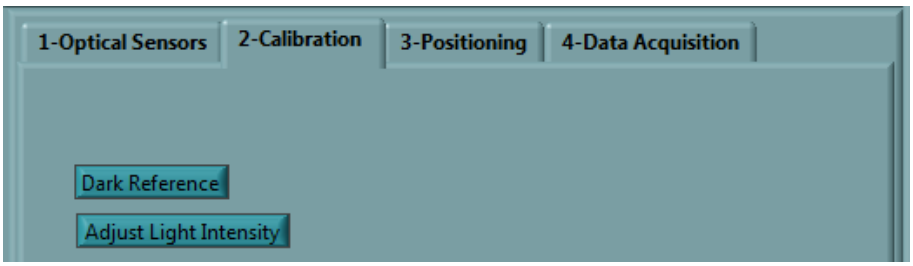

Figure 4.3: Calibration tab.

surfaces are also taken with this tab using a list of RS (see Annex 7.4). The value of 500 μm is the default value since it was the value of the RS used during the tests, but more values can be added.

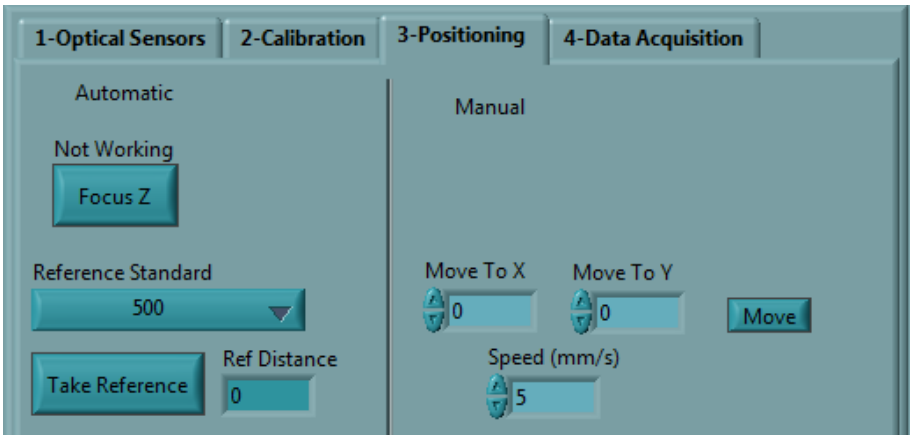

Figure 4.4: Positioning tab.

On the right side the user can control the motors with the linear position relatively to the *Home* position of each of the linear stages (see Annex 7.5).

Data Acquisition: The step before the scan is the Input of details of the sample and the structure of the data intended to receive using the data acquisition tab seen in Figure 4.5. On the left, the *Top-left Corner of First Region*, even though it's not implemented in the current version, corresponds to the reference coordinates of the first point to scan relatively to the corner of the sample.

Depending on the sample to be scanned, the number of cells, their dimensions and distance between them on the X- and Y-axis may vary. Changing the *Substeps* will change the resolution, the accuracy and the time of the scan. *Substeps* corresponds to the number of times that the ROI for both axis is divided into, e.g. for substeps=10 and ROI_X =ROI_Y =100 μm, the read positions would be for each 10 μm. If the substeps value increases, the resolution increases and the accuracy and time decrease and vice-versa. The time of the scan can be reduced by increasing the SoS, while reducing the positioning accuracy and the number of data points taken.

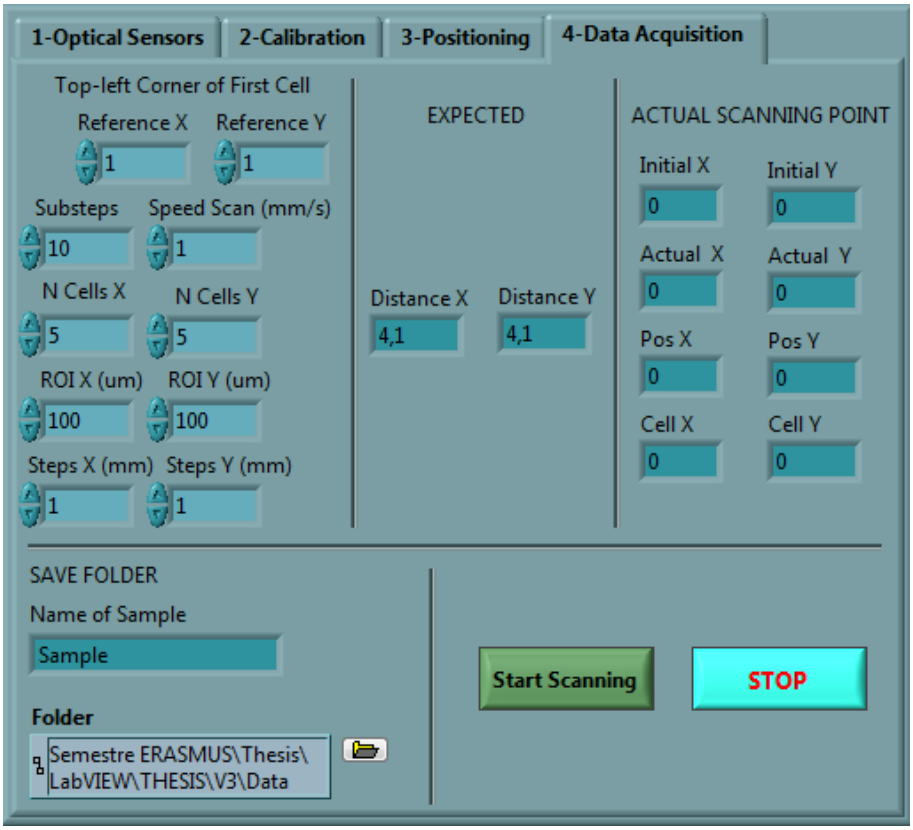

Figure 4.5: Data Acquisition tab.

In the middle column the maximum distances of measurement can be visualized accordingly to the Input data on the left column, allowing the user to be aware of the values.

On the right column, the values for *Pos X* and *Pos Y* are kept at 0 and IP and Actual Position (AP) show the relative position of the carriers to the *Home* position.

On the bottom-left of this tab the name to the sample and a folder to store the data can be chosen. On the bottom-right of this tab the acquisition of data can begin by pressing *Start Scanning*, with a previous confirmation recommended of all the Input parameters (see Annex 7.6). The values of the top-right column update when the motors move.

4.1.3 Visualization Box

After the button *Start Scanning* is pressed, the visualization box seen in Figure 4.6 waits for data of the scanned lines to be received. This box is divided in two smaller boxes: on the top one that presents the charts for visualization of the data of a cell and on the bottom a controller of which cell to visualize on the above charts. The charts can be seen simultaneously in the same tab in a smaller scale or individually in a bigger scale. The

charts are updated every time a line of a cell is read and are reset when a new cell starts to be scanned. The controls should only be used after the scan is over.

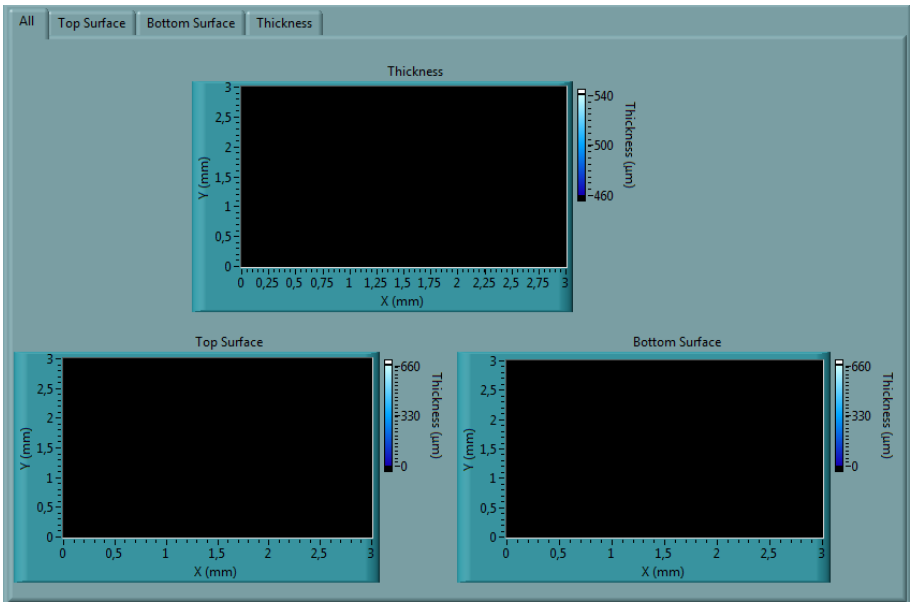

Figure 4.6: Visualization box.

4.2 Point Confocal Sensors

The PCS's were the first components tested since a major part of the main program depends on the way these sensors communicate with the computer.

4.2.1 Commands

The operation manual provides a list of different commands of which the most important ones for the project were selected in a first phase. During the development of the project and with new features to implement, other commands were added to the program (See Table 4.1).

Due to the already developed program by Tina the data communication between the sensors and the computer was kept as ASCII. All the commands start with a "$", e.g. $\$MOD$, and most of them have an answer that starts with the command and then the answer from the sensors. Some of the commands allow the usage of "?" to request the actual state/value from the sensors. In most of the algorithm the commands are used for both sensors, to make sure they have the same configuration and are working in synchronization.

ASCII Changes the output format of data to ASCII.

Data Averaging Averages the data obtained.

Table 4.1: Commands used for the PCS.

Command	Name	Function
ASC	ASCII	Telegrams in ASCII
AVD	Data Averaging	Averages Data
BIN	Binary	Telegrams in Binary
DRK	Dark Reference	Takes a Dark Reference
MOD	Mode	Measuring Mode
SCA	Scale	Distance Value
SODX	Set Output Data	Definition of Output Data
SRA	Sample Rate	Index of Sample Rate
SRI	Refractive Index	Set Refractive Index

Binary Changes the output format of data to Binary.

Dark Reference Takes a Dark Reference with the probe, in which case there should be no objects in the MR of the probe. The sensor answers with the index of the lowest possible SR.

Mode Measuring mode has 3 options: confocal for 1 surface, confocal for 2 surfaces and interferometric with indexes 0, 1 and 2, respectively.

Scale Gets the value of Full Scale in micrometers, which should be used together with the equation.

Set Output Data Selects up to 16 data words to be included in the telegram.

Sample Rate Sets the SR with indexes indexes from 3 to 7, corresponding to values of 32 (3), 100 (4), 320 (5), 1000 (6) and 2000 (7) Hz, and 127 for a free sample rate.

Refractive Index Corrects the display of thickness and dispersion Model for Modes 2 and 3.

The Baud rate is selectable only by transmitting data via the RS-232/RS-422 interface. As the data is transmitted by an USB-interface, the Baud has a maximum value of 921600.

4.2.2 PCS Algorithms

The adoption of a previously developed LV program by Tina, which is capable of measuring the distanceof the MP to the sample, helped understand the way the communication is done by the two devices. Using the functions *VISA Write* to send commands to the sensors and *VISA Read* to read the answers received is the basic process of communication. Depending on each command functionality, it is required to apply different algorithms to convert the received answer to an interface readable answer and/or to convert the user Input to a valid command.

The subVI *commands* (see Annex 7.7) sends the indicated command and reads the answer received and the subVI *CmdToValue* (see Annex 7.8) filters the unnecessary information and retrieves the numerical value of the answer. These two subVIs are used frequently together when the configuration of the sensors is changed, specially in the initialization of the sensors, where all the main configuration parameters are checked and changed if necessary to keep both sensors working at the same level.

During the acquisition of reference distances and the Scanning Cycle it is necessary to measure the distances of each surface to the corresponding sensor probe. Knowing these values it is possible to measure the thickness, if there is already a reference value taken from the RS.

To take reference values with the RS, the PCS's measure the distance of both surfaces to the corresponding sensor. To make sure the Serial is outputting the distance measured, the command SODX is sent to the sensors with the value of 1 which makes the Serial data Output as measured distances. Having both distances calculated from the average of the number of points of the SR, e.g. 1000 points, and knowing the thickness of the RS it is possible to define a RD between both sensors:

$$D_{MP} + D_{SP} + T_{RS} = RD \tag{4.1}$$

where D_{MP} and D_{SP} are the distances measured from MP to the top surface and SP to the bottom surface respectively, and T_{RS} is the thickness of the RS. During the tests the RS used had 500.0±0.1 μm[26]. If the sample is positioned in a way that the measured distance for both the Top and Bottom Surfaces is 550 μm the RD would be of 1500 μm.

During the Scanning Cycle (see Section 4.6) the distances are measured in a similar way, but another algorithm is used to retrieve the values. Due to the continuous motion, the PCS's receive a command to take an amount of values depending of the actual SR, SoS and ROI_X as:

$$\frac{SR \cdot ROI_X}{SoS} = N_{DP} \tag{4.2}$$

with N_{DP} being the Number of Data Points. In the case of these values being 1000 Hz, 1 $mm.s^{-1}$ and 100 μm, respectively, the number of values taken is 100. Using the subVI *ThicknessMeasurement* (see Annex 7.9) three arrays are obtained: one for the Top Surface distances, another for the Bottom Surface distances and a last one for the Thickness calculated using 4.1. In this case the unknown value is the thickness as the RD remains constant. These arrays are later used and explained in the Scanning Cycle Section.

4.3 Motors

In a first version of the application the Motors were used statically to make sure they were measuring at the right position and synchronized with the PCS's. However due to the time cost of this method, a continuous scanning was developed since time is one of the most important parameters for the CMM. Also the backlash and elastic deformation could affect the accuracy of the position.

The second version uses a dynamic scan, where the PCS's start acquiring data at and during the same time the motors are moving through a scanning line reducing the time factor and increasing the positioning accuracy. This method has limitations on the speed of motion, using between 1 and 5 $mm.s^{-1}$) as a recommended SoS and the initial acceleration and ending deceleration should be taken into account.

To avoid the problem of the initial acceleration, a ramp can be used, where the motor starts a certain distance away from the actual IP of the measurement which should be enough for the maximum speed to be achieved and remain constant.

Sometimes due to slopes, vibrations, SoS, limitations of the sensors or other non-predictable conditionsthe values of distance can be wrongly measured and affect the average values. It is possible to apply filters either directly in LV or use commands from the PCS that reject values out of a certain specified range and/or conditions.

The relationship between different axis is not 100% accurate so the algorithm that controls MX and MY should include a transformation Matrix in order to decrease the error. The orientation of the sample should also be identified by the positioning camera, which influence these transformed coordinates.

4.3.1 Backlash Solution

In this project there were two options thought for the removal of backlash: one through software compensation, as the backlash distance is approximately constant and dependent of the gaps between the drive and driven gears; the other by starting each scanning line by moving the motors back to the IP of the new line, instead of doing the zig-zag motion, at the cost of taking more time to finish the scan. The latter was the chosen option, since it makes it independent of the used mechanical devices, making it easier to replace the motors for different ones; in case the first option would be used, it would require changes in the LV program.

4.3.2 Motors Algorithm

With the usage of the already developed LV program *6axis_movement* by Nicoto control , up to 6 different motors, it was possible to retrieve part of the code to use in the main LV application.

The motor driver is associated with some subVI's that allow sending and receiving signals to the motors connected to it. In the *6axis_movement* program one of the basic functionalities is for the user to Input a position in *mm*. Clicking the *Send* button, the message to move to the Input position is sent to the motor driver. Then it sends a signal to the motor selected, corresponding to the rotation required by the motor so that the carrier reaches the Input linear position. While moving, the program receives data corresponding to the actual position of the stage

6 SubVIs, 2 for each motor, were created to move and check the position of the carriers: *M_move* (see Annex 7.10) and *GetPositionM* (see Annex 7.11), where M represents the x, y or z-axis motor.

The subVI *M_move* receives the position of the carrier in the M-Axis and the respective Speed of the linear translation. Through the use of other SubVIs and TMCL (Trinamic Motion Control) some steps are executed to move the motors:

1. The position in *mm* is converted to steps of rotation;
2. The axis parameters are sent with the usage of a cluster;
3. The motor starts moving to the rotational position given in 1;
4. The axis parameters are received;
5. The value returned by the hardware is converted to *mm*

The SubVI *GetPositionM* works similarly to the previously described but as it is only meant to get the actual position, the steps 1 and 2 are skipped.

Every time a motor activates, both subVIs are used to start the motion and monitor the position of the carrier until it is in the sent position.

Due to the step resolution of the motors, the value read can sometimes be different from the expected sent value, specially when it requires linear steps with a very high resolution (about 0.4 μm). For this reason, sometimes it is not possible for the carrier to stay at the expected position. To allow the cycles to stop at the right moment and avoid infinite cycles, a Step Error Compensation parameter was inserted with the value of 312.6 *nm*. For this reason, motions with a resolution inferior to 1 μm are not recommended.

As mentioned previously the motors algorithm is in the Motors Cycle. Every time the motion of a motor is required, a notification is sent from the Main Cycle to the Motors Cycle.

Move To: This notification is sent when the user wants to move the motors manually, making the Input position the actualIP. For example, if the Input is *Move To* X=20 and Y=5 *mm* a notification will be sent to the Motors Cycle and the Motors will move the carriers, first in the LSX and then in the LSY, to the positions given, with the option to change the Speed of this motion (different from SoS).

+Direction: +Direction (see Annex 7.12) acts during the phase of reading a line in a cell Cell_X (i), Cell_Y (j). It needs ROI_X, SoS, Steps_X, IP_X and actual i. The Position to Move (PTM) in the X-Axis is calculated as

$$ROI_X + IP_X + i \times Steps_X = PTM_{X_{i,j}}^{+Direction} \tag{4.3}$$

which is sent to the motors' subVIs.

Change: After a line is scanned (see Annex 7.13) the carrier moves one Substep in the Y-Axis relatively to the AP

$$AP_Y + ROI_Y/Substeps = PTM_{Y_{i,j}}^{Change} \tag{4.4}$$

and then to the initial X position of the actual scanned cell

$$IP_X + i \times Steps_X = PTM_{X_{i,j}}^{Change} \tag{4.5}$$

Change Cell X: When a cell is completely scanned, and there is at least one more cell to be scanned in the X-Axis, then the motors move the carrier (see Annex 7.14) to the initial scanning point of the new cell i+1,j with the new positions being

$$IP_X + (i+1) \times Steps_X = PTM_{X_{i+1,j}}^{Change\ Cell\ X} \tag{4.6}$$

and

$$IP_Y + j \times Steps_Y = PTM_{Y_{i+1,j}}^{Change\ Cell\ X} \tag{4.7}$$

Change Cell Y: When the last cell in the X-Axis is scanned and there is at least one more cell to be scanned in the Y-Axis, then the motors move the carrier (see Annex 7.15) to the initial scanning point of the new cell 0,j+1 with the new positions being

$$IP_X = PTM_{X_{0,j+1}}^{Change\ Cell\ Y} \tag{4.8}$$

and

$$IP_Y + (j+1) \times Steps_Y = PTM_{Y_{0,j+1}}^{Change\ Cell\ Y} \tag{4.9}$$

Exit: Stops the Motors Cycle to end the whole program.

4.4 Calibration

Due to errors of the equipment and/or modifications in the positions of the components, it is advisable and sometimes required to calibrate the program before performing scans of samples.

The MX and MY should move their respective carriers to their *Home* position, which corresponds to the linear stage minimum Position (0), before measurements. If this is not done there is the possibility of the actual read position correspond to an incorrect value, e.g. in case the motor was moved previously while turned-off. Also this can origin problems in terms of safety position, where if it moves a few *mm* more, it can damage the equipment.

The user is advised to calibrate each time the program starts although it is not mandatory. Sometimes it might be important to apply a Dark Reference and/or a White Reference as the light of the room might change, which can influence the data otherwise.

4.5 Positioning of Samples

This section describes how the Sample is positioned in the CMM before the Scanning Cycle (See Section 4.6).

4.5.1 Focus Positioning

The Positioning starts when the button *Initialize Position* is pressed. This activates the first phase, where the interface starts updating the actual distances measured by the PCS's in the Z-Axis to a RS, e.g. thickness of 500 μm inserted in the SH. It is required that the user moves the sample in the XY plane with MX and MY to a position where the focus of the PCS's is in the RS. The MP should be moved manually (as there are no motors controlling its position) up enough (about) so it doesn't interfere with the SP's MR. In case there is no stable value for the distance between the SP and the bottom surface of the RS, it means the sample is not in the MR of the sensor. As the relative distances LSZ-SP and SH-LSZ and the actual position of the carrier are known, it is possible to know the actual relative distance of the RS to the SP in the Z-Axis. This allows MZ to automatically move the SH to a position where the SR is in the SP's MR . Using the associated scale to the MP, the user can move it down (assuming it was moved up to a safe position as mentioned above) until the distance read by it has a stable value (about "600 μm"). When a good distance value is achieved a reference distance between both sensors is saved, resulted of the sum of the relative distances of both sensors to the RS's surfaces (bottom and top) with its known thickness. The individual relative distances are also saved.

After the Focus-Positioning is complete, the RS is substituted by the sample of interest and the button *Continue* should be pressed. MZ will make the SH move again in the Z-Axis, trying to find a better position for the sample of measurement, accordingly to the actual Intensities read by the PCS's: the SH will move down and up through the MR intersected by both sensors (which is known due to the relative distances of both sensors to the RS and the actual position of the SH) and in the end an algorithm selects the position with the best characteristics, to which the SH moves. These vertical positions remain the same until the end of the scan.

The previous procedures can be skipped by pressing the button *Skip* in case the Focus Positioning was done recently and the vertical positions remained unchanged.

4.5.2 XY-Positioning

The XY positioning consists of moving the sample to the preferred point to start the scan. This is done with the help of the Positioning Camera. Firstly, knowing the actual (X,Y) position, given by MX and MY and the relative distances of the Camera to the whole system, it is possible to move the sample to the focus range of the Camera. This will allow the user to see an image acquired by the camera of the top of the sample. Then the user selects the area where the starting corner appears in the image and the Camera algorithm

will identify automatically the corner by detecting lines and defining an angle between the intersection of them (the smallest one). In case the preferable corner is not in the focus range of the camera, the user can use the motors to find it and then proceed as previously described. Making use of the pixels of the image and knowing the relative distances of the Camera, it is possible to identify the orientation of the sample relatively to the system and the position point of the starting corner. After the button *Accept* is pressed MX and MY start working to move the sample to the detected point. It is common for the XY coordinate system of the sample to have a small angular difference compared to the XY coordinate system of the CMM. The knowledge of this angle (measured with the Vision Package functionalities) allows a transformation of one coordinate system to another, which will be used for the measured values during the Scanning Cycle.

4.6 Scanning Cycle

The Scanning Cycle consists of a complex synchronization of all the previously described components. This section explains how all the components work together.

The Scanning Cycle starts when the button *Start Scan* is pressed, which is only allowed after the Positioning of Samples (see Section 4.5) is executed . The Scanning Cycle can be divided in the scan of individual regions of a sample, accordingly to user Inputs. The Scanning Cycle associated to the individual regions is divided in four phases: Acceleration Ramp, Line Scanning, Next Line Positioning and Data Operations. The main cycle controls if and how the scan should continue: in the same individual region, move to another one or finish the scan.

4.6.1 Acceleration Ramp

This phase consists in moving the sample through an acceleration ramp. Knowing the actual position, that corresponds to the starting corner of the sample, using the Transformed Coordinates X'Y' , MX and MY will activate to move the corner point in an X' distance, that can depend of the Speed of Scan selected . The Acceleration Distance (AD) corresponds to the value necessary to guarantee that the carriers move with a constant speed, due to the initial acceleration of the respective motors.

4.6.2 Line Scanning

After the initial corner position of the sample is reached again, the PCS's start to acquire data over a line (see Annex 7.16) until X is the PTM as Eq. 4.3.

4.6.3 Next-Line Positioning

In case the actual Individual Region remains the same for the next scan, the sample moves in the Y-Axis as 4.4 with the help of MY and with MX the sample is moved in the X-Axis

as 4.5 (see Annex 7.17). During all of this process, the program uses an algorithm (see Annex 7.18) to average and distribute the data collected per points, update the Thickness Chart and save in a file (See Section 4.6.4).

4.6.4 Data Operations

This phase works simultaneously with the last two phases (See Sections 4.6.2 and 4.6.3). The objective is to collect the data measured by the PCS's and distribute it accordingly to the use Input preferences. The PCS's start acquiring data when the IP_X is achieved, with the command , to which is sent a certain memory space, corresponding to . When MX stops (line is complete) an algorithm is used to calculate averages over the different points in the line of the Region.

4.6.5 Change Individual Region

This phase controls if the Individual Region should change or not, how it should change and if the Scan of the whole sample is complete. Each region has the scan complete if in the last line scanned the value of Y has increased by the number of *substeps* . In this case, the algorithm checks if $\text{Cell}_i = N_{CellsX} - 1$which means all the regions of $Cell_X$ are scanned and the new PTM is as 4.6 in the X-Axis and 4.7 in the Y-Axis. In case it's not the same, the sample is moved to the next Region $Cell_X + 1$ of the same $Cell_Y$ to start its scan as 4.8 in the X-Axis and 4.9 in the Y-Axis.

Chapter 5

Results and Discussion

5.1 Acquired Data

Some data was automatically collected with the static version of the software. For a sample of Silver (Ag) produced to have 20 μm of thickness, 3 scans were made with a speed of 3 $mm.s^{-1}$, with measuring steps of 5 mm in a range of 15 mm in both X- and Y-axis. With a reference distance of 712.696 μm measured with a RS of 500.0±0.1 μm, the Table 5.1 was constructed. These values were measured from the approximate center of each cell of the sample and ideally a thickness of 20 μm should be measured in all the cell. The values for the thickness in each point should be approximately the same in the different scans. Comparing the standard deviation values in the Table 5.1, it's understood that most of the points don't have standard deviations higher than 0.2 μm, with the exception of 4 different points, that go up to 0.383 μm. Comparing the average values of the three scans with the minimum and maximum values for each point, a value of 0.815 μm is calculated as the biggest difference. This difference between the values is bigger than the expected value for the CMM, but taking into account that these values were measured with the static version, these differences can be related with some of the program characteristics: there is some acceleration immediately before the measurements, which can influence the vibrations associated; due to some backlash, that is not avoided or compensated in this version, the precision of the motion is worse, which means the probes focus in different areas.

For an easier interpretation of the data, the thickness distribution of the average of the 3 scans for each point can be seen in Figure 5.1. A darker rectangle corresponds to a higher thickness value and a lighter rectangle corresponds to a smaller thickness value. These values allow the observation of some similar tones/thicknesses, together with some extreme points.

Table 5.1: Thickness measurements for a 20 μm thickness Ag sample with the static version of the application.

X (mm)	Y (mm)	T1 (μm)	T2 (μm)	T3 (μm)	Avg (μm)	stdev (μm)
0	0	19.732	19.961	19.895	19.863	0.096
5	0	19.732	19.961	19.895	19.863	0.096
10	0	19.753	19.961	19.895	19.869	0.087
15	0	19.436	19.117	19.280	19.278	0.130
15	5	19.513	19.330	19.748	19.530	0.171
10	5	19.441	20.125	20.118	19.894	0.321
5	5	20.366	20.486	20.329	20.394	0.067
0	5	19.442	19.513	19.460	19.472	0.030
0	10	19.759	20.206	19.892	19.952	0.187
5	10	20.530	20.615	19.871	20.339	0.333
10	10	19.468	19.571	19.606	19.548	0.059
15	10	19.076	19.078	19.891	19.348	0.383
15	15	19.631	19.257	19.172	19.354	0.199
10	15	20.068	19.844	19.593	19.835	0.194
5	15	19.186	19.027	19.263	19.159	0.098
0	15	20.132	19.895	20.477	20.168	0.239

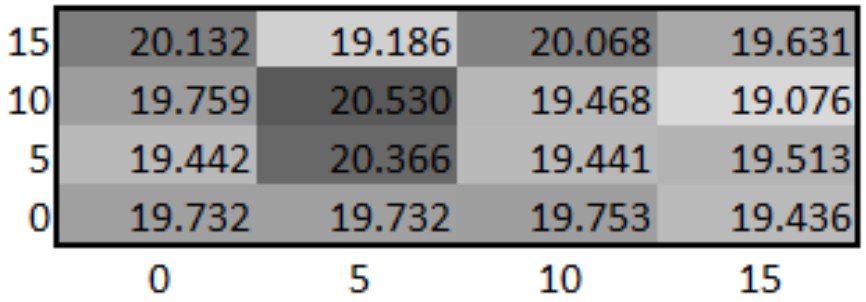

Figure 5.1: Thickness distribution chart example built in Microsoft Excel®.

Since the sample is expected to have the same thickness in the different regions, the Table 5.2 was created to compare the variation over the sample with all the data acquired. The highest value found was of 20.616 μm and the lowest was of 19.027μm, giving a range of 1.588 μm. This value is bigger than the nanometre accuracy expected but, together with the previously described influences of the static version, these difference can also come from: -the existence of some real variations in the thickness resulting from the production of the sample; -the existence of some dust; -vibrations of the whole system.

Table 5.2: Ag sample general data.

Avg	stdev	Max	Min
19.742	0.412	20.615	19.027

Chapter 6

Conclusion

During the development of the project different ideas kept adding to the standard program. Not all of them could be implemented and/or tested due to the required time to change the algorithms or need of extra hardware.

The usage of Motors' controlling subVI's that move both MX and MY simultaneously, would allow shorter paths and a faster scan.

The LV program can have a few additional features to make the usage of the system more customizable.

One feature to be implemented in a future version is the option to choose if the scan is to be done in the horizontal or vertical mode, avoiding the need of moving the sample manually. It might be important to have a sample scanned in both directions, as in the actual version the horizontal lines are averaged and in the vertical orientation there is only one value per line. Having a sample scanned in both directions and building charts with the information of both scans could give more complete data do the User.

With the addition of more constant values like relative distances and errors associated to measurements or important specifications of the different components, it becomes useful to have a dedicated file with this information editable by the User, readable by the LV program when it starts. In the interface of the main program could also exist a window or tab where the User could directly read and change these values in case some components would be substituted.

In terms of visualization a 3D image would make it easier for the User to understand the topography of the sample. It could put together the information from the actual 3 different charts from the different cells scanned, having the option to move the image in different angles. Also the option to visualize the whole sample could be implemented to better understand the distribution of the cells.

The application of filters was not yet explored in the actual version, being this possible

using the PCS's or some functions of LV. Filters can be used to remove points that are not expected due to errors and/or limitations of the whole system and/or the external environment.

The SH is expected to hold different RS in a later version, which together with the addition of a motor to move the MP in the Z-Axis would allow the measurement of samples that have a big thickness variation (the thickness varies more than theMR). Ideally it should have two different sections: an area for the samples to scan and an area for RS. Providing the relative distances of this two areas to the program, the User would just have to select the RS and not worrying about placing and removing it before each measurement. Also it would allow

The sensors have a Measuring Range of 600 μm, which imply that only until 600 μm can be measured in each half, which leaves 400 μm in height no scanned. One option is to implement a function that makes the sensor(s) get closer to the surface of the sample at each x um (for example, 500 um, to avoid extremes) using different reference samples. This can solve the problem for spheres until 10 mm diameter. However this may induce extra errors. Considering a 10 mm diameter sphere, it stays within the Working distance of the sensors, existing 1.5 mm of margin before a possible collision. There is still the problem mentioned below due to optical aperture.

In a more advanced version that involves filters and more complex data manipulation, an independent cycle for this data manipulation might be required, instead of the actual method, where the data manipulation and calculations can be done while the motors are moving to a new point. When the data manipulation takes a longer time than this motion it is important to build an independent cycle.

Chapter 7

Annexes

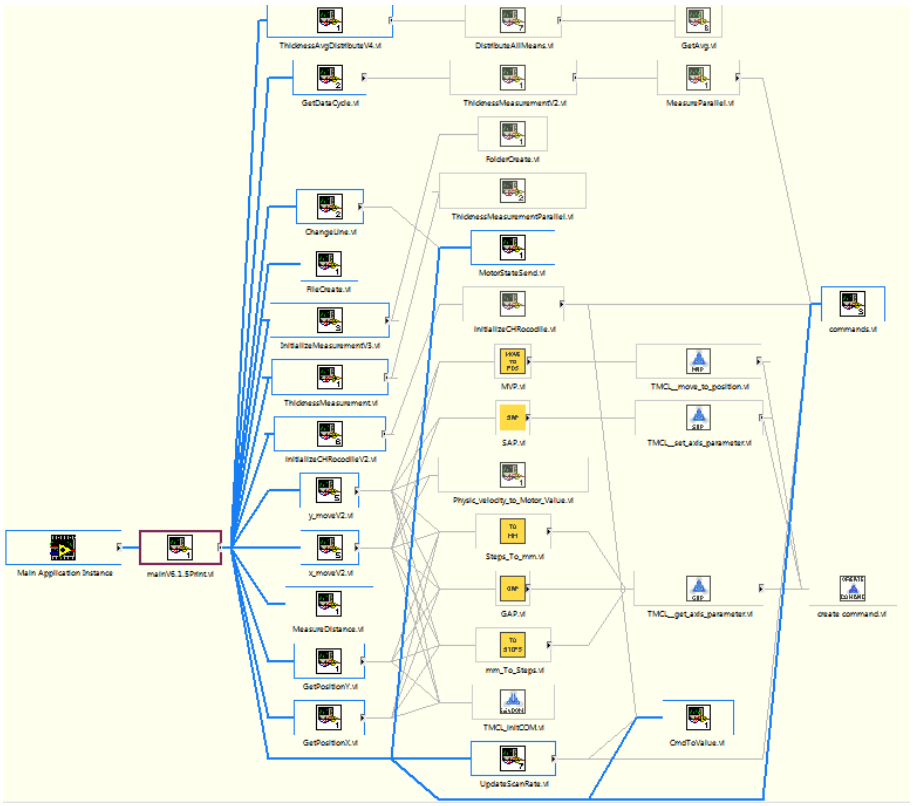

Figure 7.1: VI Hierarchy.

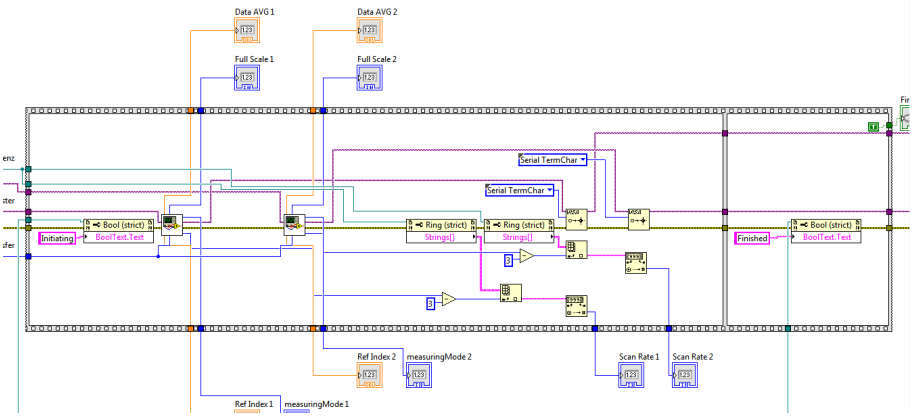

Figure 7.2: SubVI Initialize.

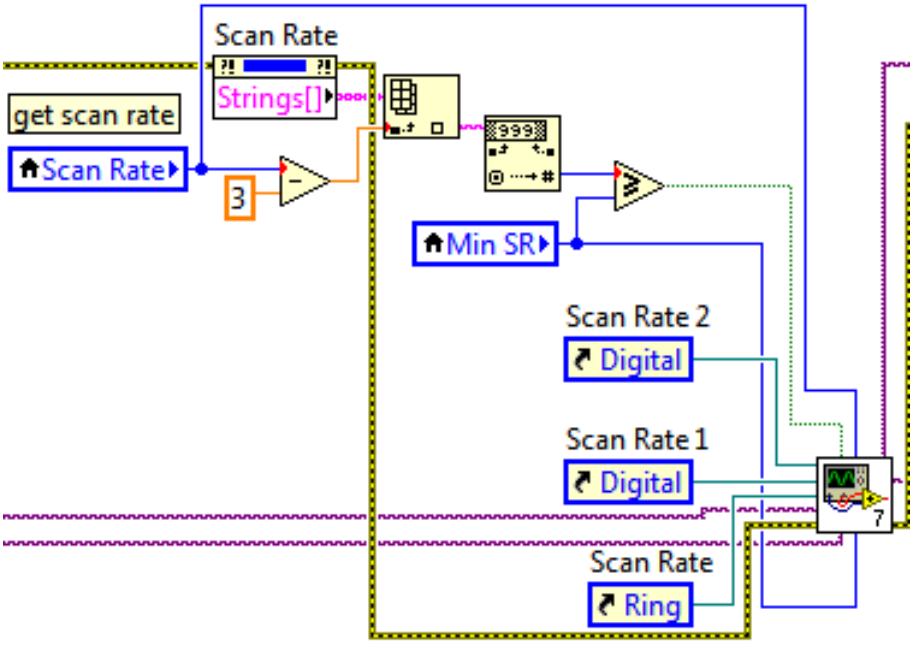

Figure 7.3: Scanning Rate algorithm.

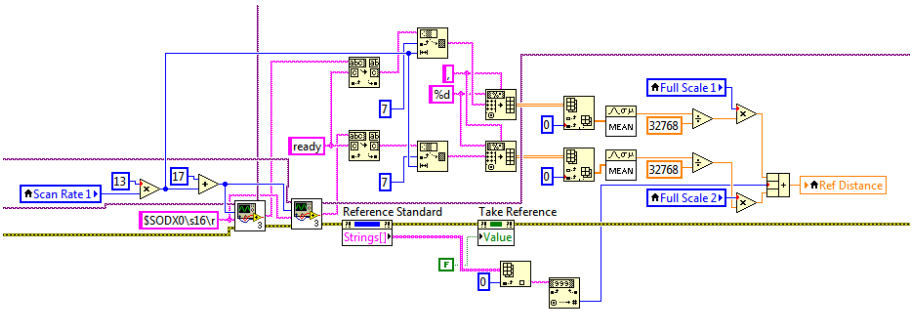

Figure 7.4: Take Reference algorithm.

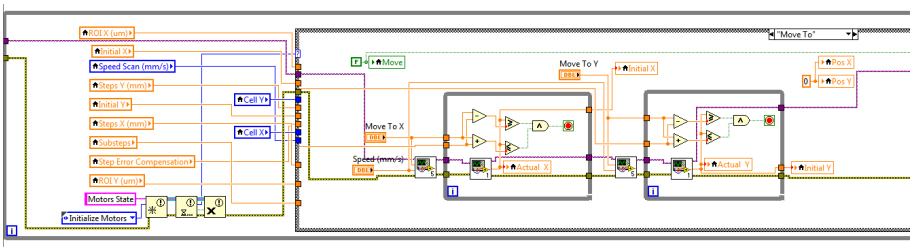

Figure 7.5: Move To algorithm.

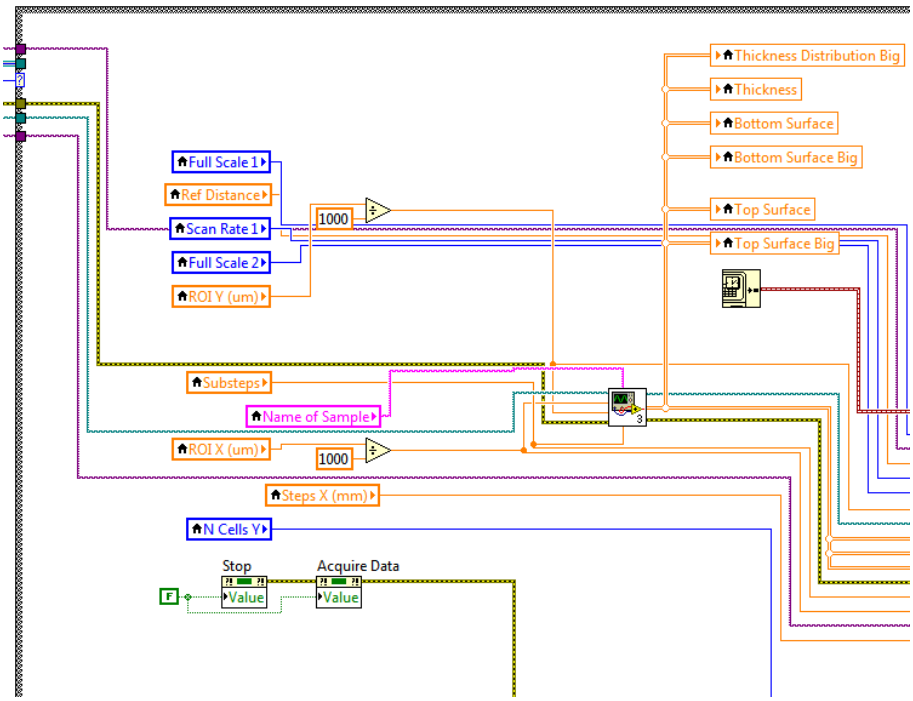

Figure 7.6: Initiate Scan algorithm.

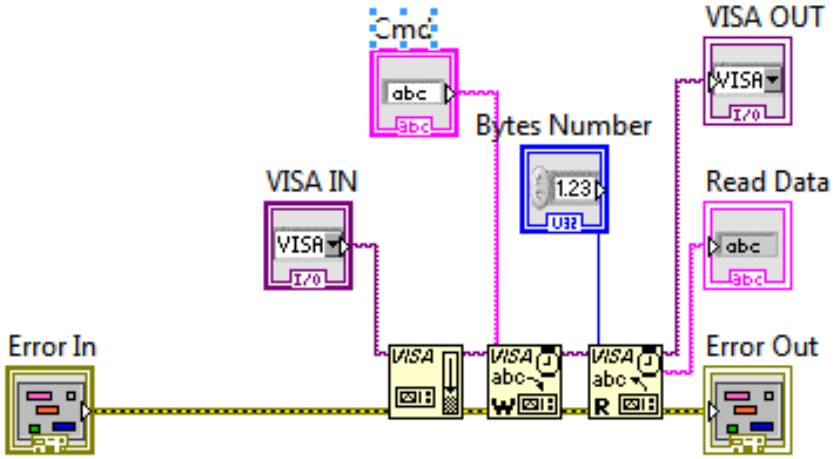

Figure 7.7: SubVI commands.

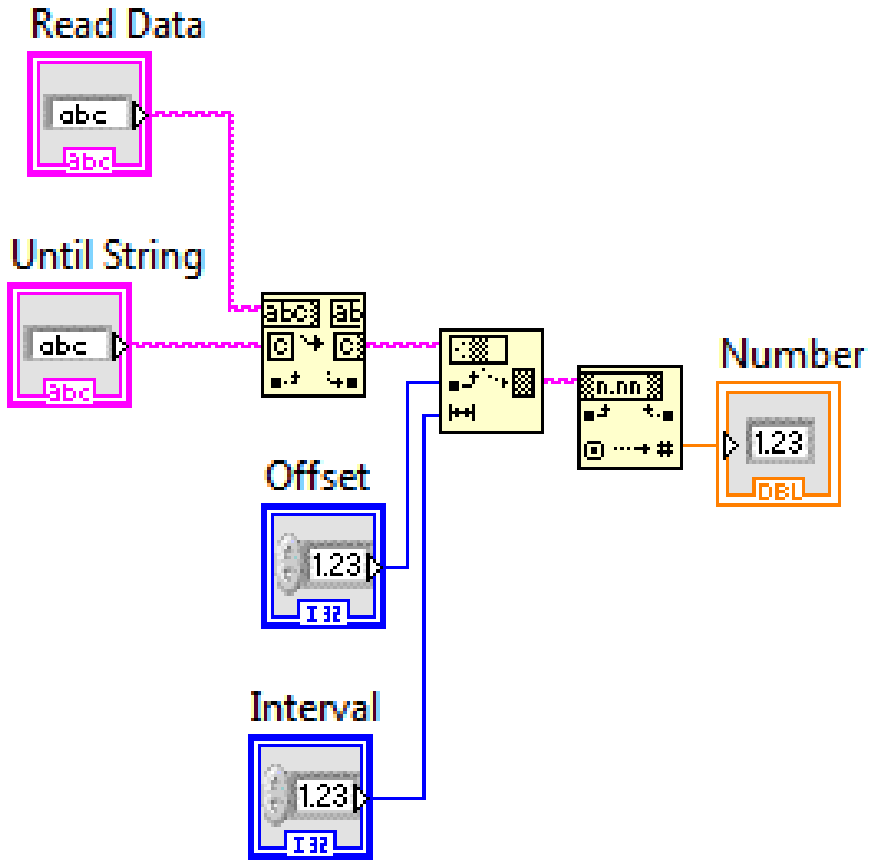

Figure 7.8: SubVI CmdToValue.

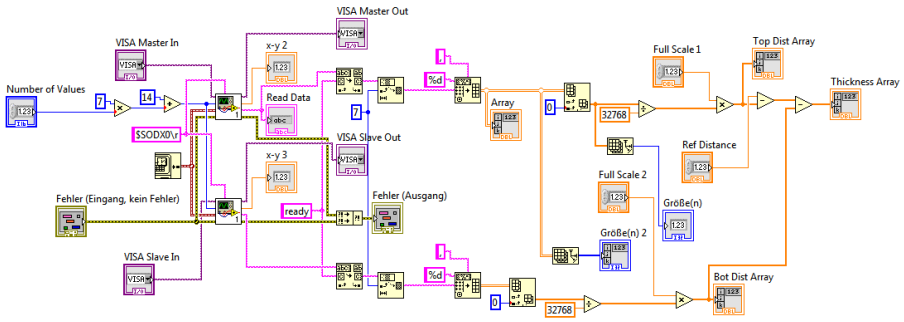

Figure 7.9: SubVI ThicknessMeasurement.

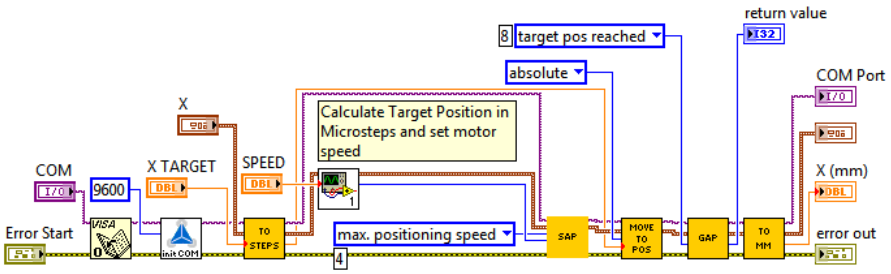

Figure 7.10: SubVI M_move for the example of M=X-axis.

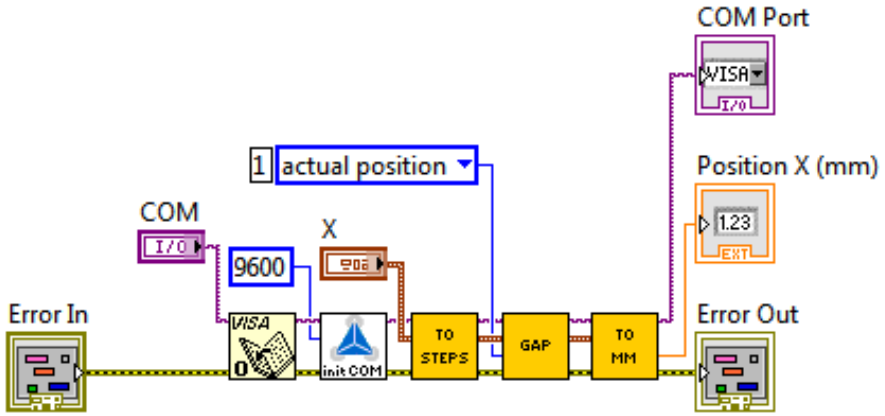

Figure 7.11: SubVI GetPositionM for the example of M=X-axis.

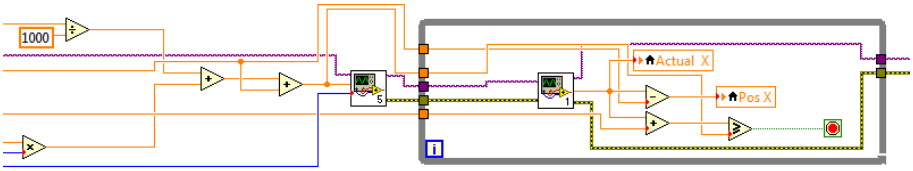

Figure 7.12: +Direction Motors algorithm.

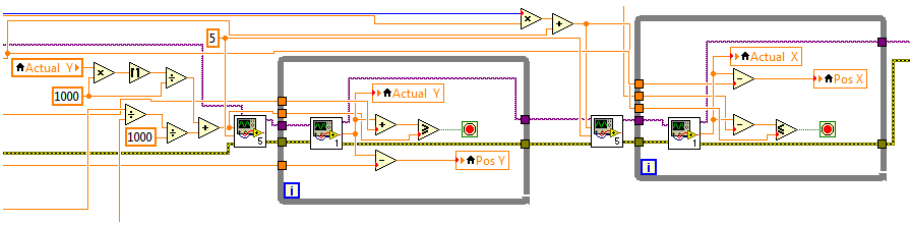

Figure 7.13: Change Motors algorithm.

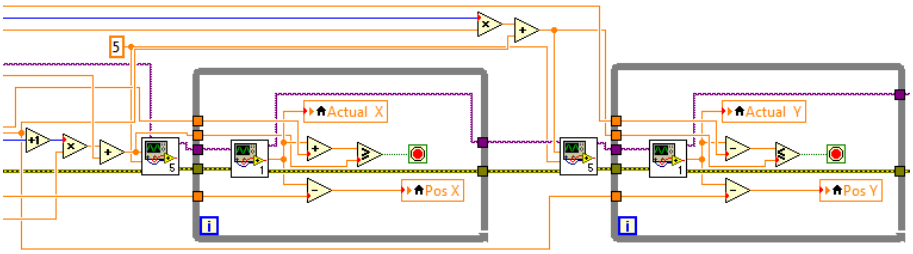

Figure 7.14: Change Cell X Motors algorithm.

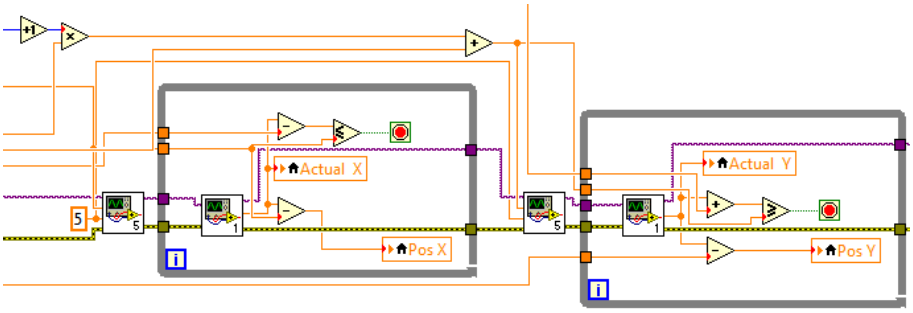

Figure 7.15: Change Cell Y Motors algorithm.

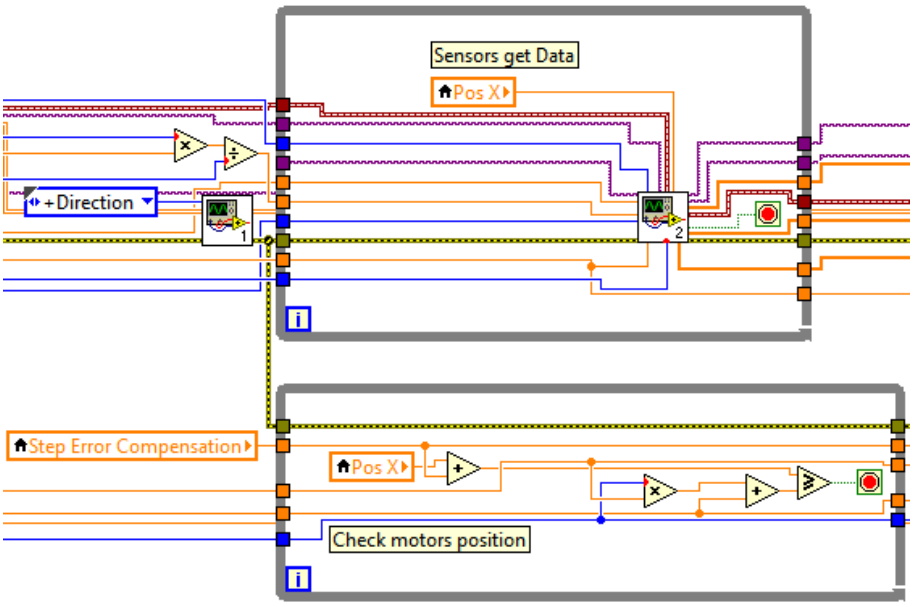

Figure 7.16: Line Scanning algorithm.

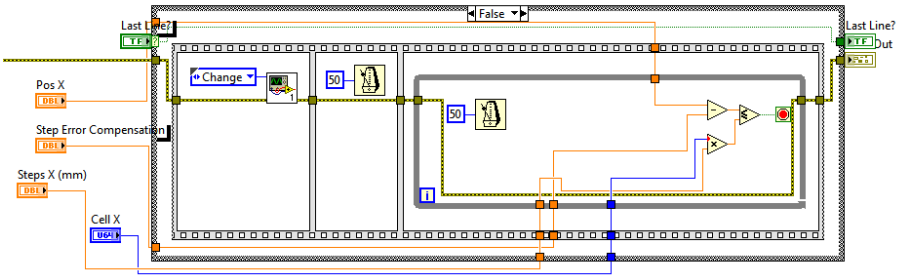

Figure 7.17: Next-Line Positioning algorithm.

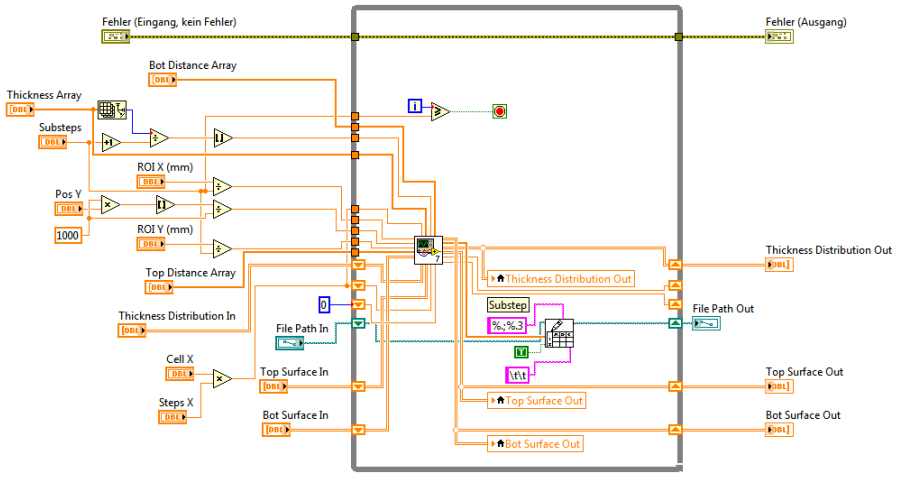

Figure 7.18: Data Operations algorithm.

Bibliography

[1] G. Schaumann. *Target Fabrication at TUD*. 2015.

[2] *PHELIX Laser System*. URL: http://www.gsi.de/phelix (visited on 03/02/2016).

[3] K. J. Stout and L. B. Blunt. *Three Dimensional Surface Topography*. 2nd Editio. Penton Press, 2000. ISBN: 1857180267.

[4] M. Conroy and J. Armstrong. "A comparison of surface metrology techniques". In: *Journal of Physics: Conference Series* 13 (2005), pp. 458–465. ISSN: 1742-6588. DOI: 10.1088/1742-6596/13/1/106.

[5] N. Tkachenko. *Optical Spectroscopy: Methods and Instrumentations*. 1st Editio. Elsevier, 2006, pp. 1–38. ISBN: 0444521267.

[6] J. L. Taylor. *The Vibration Analyisis Handbook*. First Edit. Ipp books, 1990.

[7] *Measuring Vibration*. Brüel & Kjaer, 1982. URL: http://www.bksv.com/Library/Primers.

[8] M Hillenbrand, B Mitschunas, and S Sinzinger. *Chromatic aberration theory in modern metrology*. Tech. rep. Technische Universität Ilmenau-Institut für Mikro- und Nanotechnologien, 2009.

[9] A. Miks, J. Novak, and P. Novak. "Analysis of method for measuring thickness of plane-parallel plates and lenses using chromatic confocal sensor." In: *Applied optics* 49.17 (2010), pp. 3259–3264. ISSN: 0003-6935. DOI: 10.1364/AO.49.003259.

[10] Precitec Optronik GmbH. *Optical Sensor CHRocodile S Operation Manual*. 2015.

[11] *CHRocodile S/SE Sensor*. URL: http://www.precitec.de/en/products/optical-measuring-technology/chromatic-confocal-sensors/chrocodile-s-se/ (visited on 03/01/2016).

[12] B. Schweber. *Stepper Motors Make the Right Moves with Precision , Ease and Smarter Drivers*. URL: http://eu.mouser.com/applications/stepper-motors-smart-drivers/ (visited on 09/02/2016).

[13] *Stepper Motor Guide*. URL: http://www.anaheimautomation.com/manuals/forms/stepper-motor-guide.php (visited on 09/02/2016).

[14] Circuitspecialists. *Stepper Motor Basics*. URL: https://www.circuitspecialists.com/stepper-motor (visited on 08/20/2016).

[15] FAULHABER. *How to Select a DC Micromotor*.

[16] MICROMO. *Stepper Motor Technical Note: Microstepping Myths and Realities*.

[17] SmarAct. *Linear Positioners*. URL: http://www.smaract.com/products/linear-positioners (visited on 04/20/2016).

[18] M. Mateen. "How to make a Motorized Linear Translation Stage". In: (2009).

[19] *Encoder Guide*. URL: http://www.anaheimautomation.com/manuals/forms/encoder-guide.php (visited on 09/02/2016).

[20] *Understanding Resolution in Optical and Magnetic Encoders*. URL: http://electronicdesign.com/components/understanding-resolution-optical-and-magnetic-encoders (visited on 06/15/2016).

[21] Danaher Industrial Controls. *Encoder Application Handbook*. 2003.

[22] *Piezoelectric Effect*. URL: https://www.comsol.com/multiphysics/piezoelectric-effect (visited on 09/01/2016).

[23] J. Broch. *Mechanical Vibration and Shock Measurements*. Brüel & Kjaer, 1984, pp. 97–128. ISBN: 8787355345.

[24] *Measuring Vibration with Accelerometers*. URL: http://www.ni.com/white-paper/3807/en/ (visited on 05/13/2016).

[25] I. Bell. *Introduction to Basic LabVIEW Design Patterns*. National Instruments, 1993.

[26] *PTB*. URL: https://www.ptb.de/ (visited on 05/28/2016).